CATALYSTS FOR ULTRAHIGH CURRENT DENSITY OXYGEN CATHODES FOR SPACE FUEL CELL APPLICATIONS

Final Report - February 1, 1989 to April 30, 1991

Principal Investigators:

D. Tryk, Senior Research Associate

E. Yeager, Hovorka Professor of Chemistry

Research Personnel:

M. Shingler, Postdoctoral Research Associate

W. Aldred, Research Assistant

C. Wang, Visiting Scholar

Z. Zhang, Graduate Student

Case Center for Electrochemical Sciences

and the Chemistry Department

Case Western Reserve University

Cleveland, Ohio 44106-7078

Research sponsored by the NASA Lewis Research Center

Grant No. NAG3-694

September 30, 1991
(revised January 13, 1992)

TABLE OF CONTENTS

I. SUMMARY

The objective of this research was to identify promising electrocatalyst/support systems for oxygen cathodes capable of operating at ultrahigh current densities in alkaline fuel cells. Such cells will require operation at relatively high temperatures and O_2 pressures. A number of materials were prepared, including Pb-Ru and Pb-Ir pyrochlores, RuO_2 and Pt-doped RuO_2, lithiated NiO and La-Ni perovskites. Several of these materials were prepared using techniques that had not been previously used to prepare them. Particularly interesting was the use of the alkaline solution technique to prepare Pt-doped Pb-Ru pyrochlores in high area form. Also interesting was the use of the fusion (melt) method for preparing the Pb-Ru pyrochlore. Several of the materials were also deposited with platinum.

Well-crystallized $Pb_2Ru_2O_{7-y}$ was used to fabricate very high performance O_2 cathodes with good stability in room temperature KOH. This material was also found to be stable over a useful potential range at ~140°C in concentrated KOH. For some of the samples, fabrication of the gas-fed electrodes could not be fully optimized during this project period. Future work may be directed at this problem. Pyrochlores that were not well-crystallized were found to be unstable in alkaline solution.

Very good O2 reduction performance and stability were observed with Pb2Ru2O7-y in a carbon-based gas-fed electrode with an anion-conducting membrane placed on the electrolyte side of the electrode. The performance came within a factor of about two of that observed without carbon.

High area platinum and gold supported on several conductive metal oxide supports were examined. Only small improvements in O_2 reduction performance at room temperature were observed for $Pb_2Ru_2O_{7-y}$ as a support because of the high intrinsic activity of the pyrochlore. In contrast, a large improvement was observed for Li-doped NiO as a support for Pt. Very poor performance was observed for Au deposited on Li-NiO at ~150°C.

Nearly reversible behavior was observed for the O_2/OH^- couple for Li-doped NiO at ~200°C. The temperature dependence for the O_2 reduction was examined.

II. INTRODUCTION AND OBJECTIVES

Improvements in the performance of the oxygen cathode in alkaline fuel cells can lead to major improvements in the overall operation of such cells. The areas in which improvements can be made include the electrocatalysis, the electrode structure and the electronic conductivity. The achievement of ultrahigh current densities will rely on all three aspects, particularly the optimization of mass transport and electronic conductivity. The stability of the catalyst and electrode structure is also of utmost importance.

The objective of this research was to identify promising electrocatalyst/support systems for oxygen cathodes capable of ultrahigh current density operation in alkaline fuel cells operating at relatively high temperatures and O_2 pressures. The research has focused on the preparation and characterization of candidate catalyst/support systems offering high catalytic activity, electronic conductivity and physical/chemical stability.

Significant progress was made in the preparation and evaluation of transition metal oxide materials both as catalyst supports and catalysts in their own right. Methods have been developed to fabricate some of these oxides into PTFE-bonded gas-fed electrodes with high performance. A number of electrodes were examined at relatively high temperatures (~140-150°C) in concentrated KOH. The stability of the well-crystallized lead ruthenate pyrochlore $Pb_2Ru_2O_{6.5}$ was found to be quite encouraging. Lithiated nickel oxide electrodes were examined at temperatures as high as ~225°C. The performance of these electrodes was good over the range 200-225°C.

A number of new compounds were synthesized, including platinum-doped lead ruthenate pyrochlore and platinum-doped RuO_2. The preparation of highly dispersed platinum and gold on conductive metal oxide supports, including Pb2Ru207-y, and Li-NiO was undertaken. Platinum on Li-NiO showed excellent performance at ~150°C, while gold on Li-NiO showed poorer performance than the unadorned oxide.

The choice of candidate support materials was guided by considerations of 1) stability in concentrated alkaline solution over the range of potentials expected to be operative for the high performance fuel cell and 2) high electronic conductivity, preferably at least 10^2 $(\Omega\ cm)^{-1}$. The materials receiving the most attention were lead ruthenate and iridate pyrochlores, RuO_2 and Ir-substituted RuO_2, and lithiated NiO. The nickel-based perovskites $LaNiO_3$ and La_2NiO_4 were prepared in relatively low area form. La_2NiO_4 is a layered-type perovskite, which is related structurally to the oxide superconductors.

III. EXPERIMENTAL METHODS

A. Preparation of Metal Oxide Catalysts and Supports

1. Pyrochlores and ruthenium oxides

Lead-ruthenium and lead-iridium pyrochlores were prepared using the alkaline solution precipitation method developed by Horowitz et al. (1-5) as well as a CWRU-developed modification of this method. The Horowitz method (hereafter refered to as the alkaline solution method) utilizes an alkaline solution both as a means of reacting the metal ions by precipitation to form an amorphous pyrochlore precursor and subsequently as a medium for the crystallization of the precipitate.

Table 1 provides a list of the pyrochlores and other ruthenium and iridium-based oxides prepared for this project. The heat treatment temperatures and times are given together with the BET surface areas and the approximate resistivities in some cases. In an effort to establish the effects of variations in the prepation conditions on the physical and chemical properties, these conditions are given in Appendix 1. In ongoing work at CWRU, this database will be continued and will be extended to include data from other laboratories.

The first step in the typical preparation technique was to mix solutions of the cations in the proper stoichiometric ratio. Stock solutions were made with the following compositions: 0.025 M Ru (chloride), 0.025 Ir (chloride), and 0.025 M Pb (acetate). After mixing, the solutions were typically stirred and heated to 60 - 70°C. Oxygen gas was bubbled into the solutions, and KOH solution was slowly

Table 1
Ruthenium and Iridium-Based Transition Metal Oxides Prepared for this Project

	compound	method	BET area $m^2 g^{-1}$	HT[a] temp. °C	HT[a] time h	structural characteristics based on XRD
	Pb-Ir compounds					
1.	$Pb_2Ir_2O_{7-y}$	alk. sol.	1.6	407	18	crystalline
2.	$Pb_2Ir_2O_{7-y}$	alk. sol.	4.3	407	18	crystalline
3.	Pb-Ir oxide	alk. sol.	47.8	195	16	amorphous
4.	Pb-Ir oxide	alk. sol.	66.0	90	4	amorphous
	Pb-Ru compounds					
5.	$Pb_2Ru_2O_{7-y}$	alk. sol.	11.6	none	none	crystalline
6.	$Pb_2Ru_2O_{7-y}$	alk. sol.	11.4	300	24	cyrstalline
7.	$Pb_2Ru_2O_{7-y}$	alk. sol.	21.4	407	18	crystalline, (some RuO_2)
8.	$Pb_2Ru_2O_{7-y}$	alk. sol.	43.5	407	18	crystalline (some RuO_2)
9.	$Pb_2Ru_2O_{7-y}$	NO_3^- melt	3.1	500	2	crystalline
10.	$Pb_2Ru_2O_{7-y}$	alk. sol.	104.6	90	4	poorly cr. (very broad peaks)
11.	$Pb_2Ru_2O_{7-y}$	alk. sol.	56.1	195	16	crystalline
12.	$Pb_2Ru_2O_{7-y}$	alk. sol.	54.8	205	18	-
13.	$Pb_2Ru_2O_{7-y}$	alk. sol.	66.1	205	18	-
14.	$Pb_2Ru_2O_{7-y}$	alk. sol.	36.9	205	18	-
15.	$Pb_2Ru_2O_{7-y}$	alk. sol.	10.6	205	18	-
16.	$Pb_2Ru_2O_{7-y}$	alk. sol.	49.8	200	16	crystalline
17.	$Pb_2Ru_2O_{y-y}$	alk. sol.	3.5	600	4	crystalline
	Pb-Ru-Pt compounds					
18.	$Pb_2Ru_{1.98}Pt_{0.02}O_{7-y}$	alk. sol.	64.4	205	18	amorphous
19.	$Pb_2Ru_{1.905}Pt_{0.095}O_{7-y}$	alk. sol.	72.1	210	16	amorphous
20.	$Pb_2Ru_{1.98}Pt_{0.02}O_{7-y}$	alk. sol.	51.5	200	16	crystalline
21.	$Pb_2Ru_{1.9}Pt_{0.1}O_{7-y}$	alk. sol.	47.6	-	-	crystalline
22.	$Pb_2Ru_{1.8}Pt_{0.2}O_{7-y}$	alk. sol.	67.7	-	-	crystalline

(continued on next page)

Table 1 (continued)
Ruthenium and Iridium-Based Transition Metal Oxides Prepared for this Project

	compound	method	BET area $m^2 g^{-1}$	HT[a] temp. °C	HT[a] time h	structural characteristics based on XRD
23.	$Pb_2Ru_{1.98}Pt_{0.02}O_{7-y}$	alk. sol.	2.6	600	4	crystalline
24.	$Pb_2Ru_{1.94}Pt_{0.06}O_{7-y}$	alk. sol.	3.8	600	4	crystalline
25.	$Pb_2Ru_{1.9}Pt_{0.1}O_{7-y}$	alk. sol.	3.1	600	4	crystalline
	Ru-O_2-based compounds					
26.	RuO_2	th. decomp.	6.3	500	3	-
27.	RuO_2	NO_3^- melt	8.0	500	3	crystalline
28.	RuO_2	alk. sol.	66.4	205	16	amorphous
29.	$Ru_{0.98}Pt_{0.02}O_2$	alk. sol.	68.1	205	16	amorphous
30.	$Ru_{0.9}Pt_{0.1}O_2$	citrate	-	700	1	cr., not rutile[b]
31.	$Ru_{0.5}Pt_{0.5}O_2$	citrate	-	700	1	cr., not rutile[b]
	Ru-containing perovskites					
32.	$SrRuO_3$	OH^- ppt.	10.7	407	18	-
33.	$CaRuO_3$	OH^- ppt.	28.2	407	18	-

a. Abbreviations: HT = heat treatment; alk. sol = alkaline solution; th. decomp. = thermal decomposition; ppt. = precipitation; cr. = crystalline.
b. These compounds were crystalline but were not the expected RuO_2 rutile crystal structure.

added until a controlled pH between 12 and 14 was reached. This procedure differed from the typical Horowitz procedure because, in the CWRU modification, the metal salt solutions were made up and used for several syntheses. This made it more convenient to carry out the syntheses, because the solutions were simply measured out volumetrically and then mixed.

In many of the CWRU syntheses, the KOH solution was added to the mixture of metal salt solutions (e.g., Pb and Ru), and the pH was slowly increased. In the preferred Horowitz procedure, the metal salt solution was added to a KOH solution so that the metal ions immediately were exposed to the desired pH. In one of the CWRU syntheses, the Pb salt was dissolved in KOH solution, and then the Ru salt solution was slowly added. This soltion was then allowed to react for about 48 h. As discussed later, this compound was very well crystallized and consisted mostly of small single crystals.

After filtering and washing, the precipitates were dried and in some cases not heat-treated further. In other cases the samples were heat-treated at temperatures up to 600°C in air for times up to 24 h.

Molten salt or fusion-type preparative methods were also examined. Methods that make use of alkali metal chloride melts have been employed to prepare $LiAlO_2$ (6), $SrTiO_3$ (7) and a number of electronically conductive oxides for use as cathodes in molten carbonate fuel cells (8). Nitrate melts have been used to prepare RuO_2-IrO_2 solid solutions in high area form, from 40 to 90 $m^2\ g^{-1}$ (9). These methods involve the reaction of the precursor metal salts as dissolved species in the molten salt to form a dissolved product (6). If the melt is cooled quickly, th product is at a very high state of dispersion and uniformity of

composition. It is recovered by dissolving out the water-soluble alkali metal chloride or nitrate.

The method for preparing the RuO_2-IrO_2 solid solutions consisted of mixing appropriate quantities of iridium chloride and/or ruthenium chloride with $NaNO_3$ in a 1:5 weight ratio of the chlorides to the $NaNO_3$ (9). This mixture was then melted and held at 500°C for 3 hours. When the sample had cooled, the nitrate was dissolved in distilled water, and the oxide was filtered out. After the filtered powder was dried, it was then heat-treated at 550°C for one hour.

This procedure was used to make pure RuO_2 (compound 1-27). It was also modified to produce $Pb_2Ru_2O_{6.5}$ (compound 1-9) by adding the appropriate amount of lead acetate to the ruthenium chloride and adjusting the amount of $NaNO_3$ so that the weight ratio of combined ruthenium and lead salts to $NaNO_3$ remained 1:5.

2. Platinum-substituted ruthenium-based oxides

Methods were developed to dope $Pb_2Ru_2O_{6.5}$ and RuO_2 with platinum based on the alkaline solution method. In principle, the platinum should then exist as an integral part of the oxide structure at an atomic level of dispersion. The Pt would substitute for Ru in the pyrochlore structure. It is not known whether or not the Pt would be subsequently electrochemically reduced during operation as an O_2 cathode. Some Pt oxide compounds such as the Pt bronzes, however are known to be stable in the O_2 reduction potential range (26), forming either small Pt metal clusters or isolated Pt metal atoms. The following compositions were prepared: $Pb_2Ru_{1.98}Pt_{0.02}O_{7-y}$,

$Pb_2Ru1.94Pt0.06O7-y$, $Pb_2Ru1.905Pt0.095O7-y$, $Pb_2Ru1.9Pt0.1O7-y$, $Pb_2Ru1.8Pt0.2O7-y$, RuO_2 and $Ru_{0.98}Pt_{0.02}O_2$, although it should be noted that these compositions have not been confirmed via analysis. These were prepared via the alkaline solution technique, where the pH for the pyrochlore compositions was adjusted to 12-13 and that for the RuO_2 composition to 10.5 $\pm$ 0.1. The solutions used for these preparations were as follows: 0.025M ruthenium chloride, 0.025 M lead acetate and 0.025 M chloroplatinic acid. The appropriate volume ratios of these solutions were mixed to yield the desired oxide compositions.

For some of the samples, the aqueous solutions containing the appropriate metal ions were heated for 3 h at 65°C with O_2 gas bubbling through them. This is very similar to the processing procedure that was done on prior batches of crystalline $Pb_2Ru_2O_{6.5}$. The solutions for the RuO_2 compositions were heated at 45°C for 2 h with no gas bubbling. All powders were filtered, washed with water, dried at 90°C for 3 h and heated in air at 195-210°C for 16-18 h. The above procedure produced $Pb_2Ru_2O_{7-y}$ (compound 1-11) with the pyrochlore crystal structure and a BET area of 56.1 $m^2\ g^{-1}$. The RuO_2 and Pt-doped RuO_2 (compounds 1-28 and 1-29 respectively) had relatively high areas (66.4 and 68.1 $m^2\ g^{-1}$) but were amorphous.

The oxides RuO_2, $Ru_{0.9}Pt_{0.1}O_2$ and $Ru_{0.5}Ir_{0.5}O_2$ were prepared via the citric acid decomposition method (discussed in III.A.3.). This was done by adding one mole of citric acid and urea for every mole of the metal cations in the solution. Then these solutions were stirred and dried in a drying oven. The char residue was then heated in a furnace at ~600°C for 4 h.

3. Lithiated nickel oxide and nickel-based perovskites

Lithiated nickel oxide samples with Li contents of 0 to 10 at.% were prepared using a variety of methods, including the thermal decomposition, freeze-dry and citrate methods (see Table 2). Further preparative details are provided in Appendix 2. The citrate method(s) included the citric acid-ethylene diamine process used by Chen and Anderson (10) to prepare Y-Ba-Cu perovskites as well as a CWRU-developed modification of this method where urea was substituted for ethylene diamine. The latter method involved the formation of an organic gel based on citric acid and urea together with the Ni(II) acetate and Li carbonate. The citric acid and urea were present in a mole ratio in excess of unity with respect to the combined total of Ni and Li. This method is partly based on the work of Sale and coworkers on the "amorphous citrate" process for preparing perovskites and other oxides (11). In the present work, a series of compounds, including undoped NiO, three Li-doped NiO samples and two La-Ni perovskites, was prepared. The citrate method was used to prepare these perovskites. Unfortunately the surface areas were low.

One problem with the citrate methods is that a certain amount of amorphous carbon is produced. This was observed in the TEM of one of the Li-doped NiO samples. Further heat treatments at elevated temperatures in air are required to oxidize this carbon, and this treatment can lead to loss of surface area of the oxide.

The highest area NiO samples were prepared via the thermal decomposition of nickel hydroxide and nickel carbonate in vacuo at relatively low temperatures (<300°C). The BET areas were 80 and 60 m^2

Table 2
Nickel-Based Oxides Prepared for this Project

compound[b]	method	BET area $m^2 g^{-1}$	HT[a] temp. °C	HT[a] time h	structural characteristics based on XRD
NiO-based compounds					
1. NiO	citrate	-	800	10	-
2. $Ni_{0.98}Li_{0.02}O$	citrate	-	800	10	-
3. $Ni_{0.96}Li_{0.04}O$	citrate	-	-	-	-
4. $Ni_{0.94}Li_{0.06}O$	citrate	-	650	24	-
5. NiO	citrate	-	650	24	crystalline
6. $Ni_{0.96}Li_{0.04}O$	citrate	-	650	24	crystalline
7. $Ni_{0.9}Li_{0.1}O$	citrate	0.86	650	24	crystalline
8. $Ni_{0.95}Li_{0.05}O$	citrate	9	500	12	crystalline
9. $Ni_{0.95}Li_{0.05}O$	citrate	1	600	12	crystalline
10. $Ni_{>0.99}Li_{<0.01}O$	OH^- ppt.	80	260	18	crystalline
11. $Ni_{0.98}Li_{0.02}O$	freeze dry	2	450	5	incomplete rx
12. $Ni_{>0.99}Li_{<0.01}O$	CO_3^{2-} ppt.	60	290	18	crystalline
13. $Ni_{0.9}Li_{0.1}O$	NO_3^- decomp.	2.5	650	30	crystalline
14. Cr-doped NiO	NO_3^- decomp.	NA	650	30	crystalline
Ni-containing perovskites					
15. $LaNiO_3$	CO_3^{2-} decomp.	NA	900	24	crystalline, tr. La_2O_3, NiO
16. La_2NiO_4	CO_3^{2-} decomp.	NA	1200	12	cr., tr. La_2O_3
17. $LaSr_{0.75}Ba_{0.25}NiO_4$	CO_3^{2-} decomp.	NA	1200	12	crystalline
18. $La_4Ni_3O_{10}$	CO_3^{2-} decomp.	NA	1200	24	crystalline
19. La_2NiO_4	citrate	2	900	12	crystalline, tr. La_2O_3, NiO
20. $LaNiO_3$	citrate	NA	900	24	crystalline, tr. La_2O_3, NiO

a. Abbreviations: HT = heat treatment; ppt. = precipitation; tr. = trace; decomp. = decomposition; cr. = crystalline; NA = not available; rx = reaction.

b. Note that the compositions have not been confirmed by analysis.

g^{-1} respectively. Lithium acetate was present in the mixture in order to try to incorporate Li^+ ions during this procedure. Unfortunately, however, the amounts of Li incorporated were very small, and resistivities were very large (>10^5 Ω cm). Further work will be carried out at CWRU to prepare high area Li-doped NiO using new methods that have recently become available.

B. Preparation of Highly Dispersed Platinum on Metal Oxide Supports

In addition to the materials above in III.A.2, which have platinum incorporated into the bulk structure, platinum was also deposited on oxide supports using the Prototech method, which involves the decomposition of the sulfite complex of platinum with hydrogen peroxide in the presence of an aqueous suspension of the support material (12). This precipitates a platinum hydroxide colloid. After filtering and washing the samples, they were dried in air at ~150°C. No reduction step was employed. The Pt hydroxide undergoes reduction when the catalyst is used in an electrode at O_2 reduction potentials.

C. Physical Characterization

X-ray diffraction was carried out on most of the samples, using the Philips diffractometer in the Materials Science Department at CWRU. BET surface area measurments were made using the Leeds and Northrup automatic BET analyzer at NASA-Lewis. Scanning electron microscopy was done on some samples using the JEOL SEM instrument at the Macromolecular

Sciences Department at CWRU. Transmission electron microscopy was done on the Philips 400T instrument in the Materials Science Department at CWRU.

For doing the conductivity measurements, a conductivity cell for powder samples was fabricated. The design (Fig. 1) is similar to designs that have been described in the literature (13, 14) and consists of a non-conductive die body, in this case, Macor machinable ceramic (Corning), and stainless steel pistons. A constant current was applied across the pistons, and the voltage drop was measured across two silver voltage probes that were inserted into the die body. The latter were at a fixed distance of 0.44 cm from each other. The cross-sectional area of the cavity was 0.248 cm^2.

D. Fabrication of Porous Electrodes

The procedure for the fabrication of porous Teflon-bonded gas-fed electrodes based on metal oxides for O_2 reduction measurments is briefly as follows.

A sample of 100-200 mg of the oxide was mixed ultrasonically for five minutes in 30 cm^3 of deionized water. Magnesium sulfate (200 mg) was added to increase ionic strength and to aid in the coagulation of the Teflon emulsion (subsequently added). A measured volume of pre-diluted Teflon suspension (2-3 % w/v) was further diluted by a factor of ~10 and was added to obtain 25 wt% Teflon solids based on the total weight of oxide plus Teflon. The PTFE suspension was diluted from a commercially available emulsion, DuPont Teflon T30B. The mixture was then ultrasonically blended for 15 minutes. After removing from the

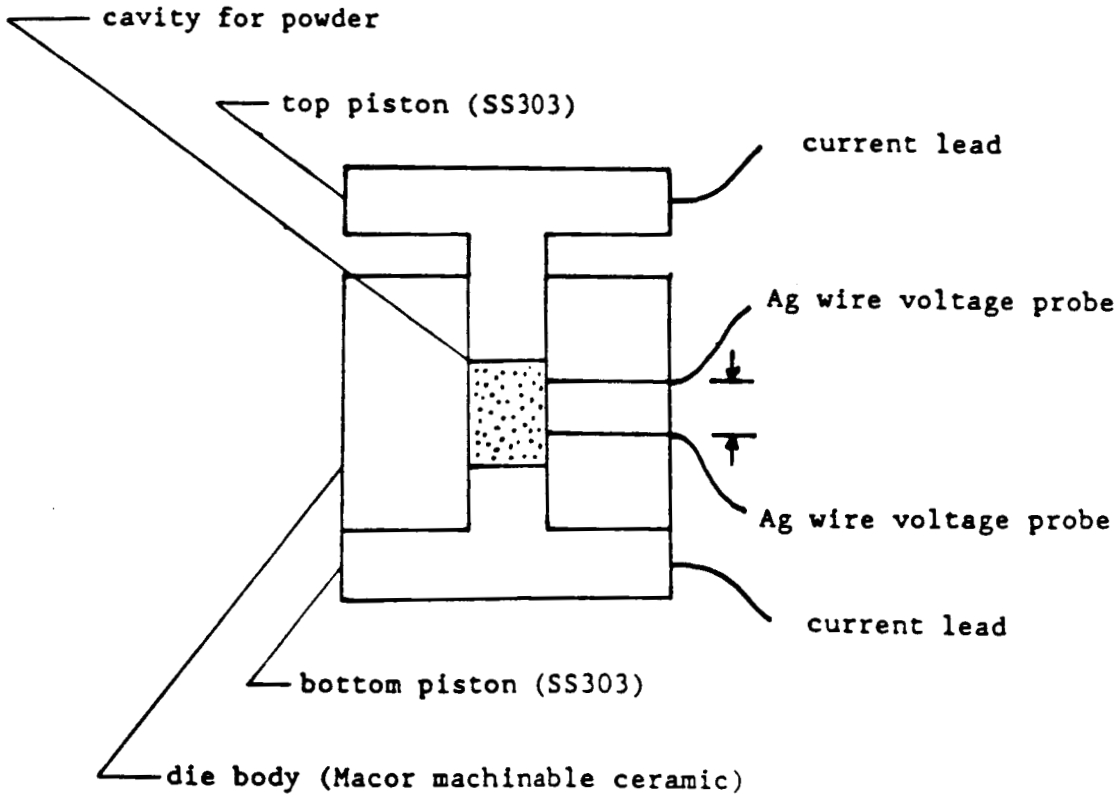

Fig. 1. Conductivity cell for powder samples under pressure loads, based on Beyerlein et al. (13) and Espinola et al. (14).

ultrasonic bath, the material was filtered and washed thoroughly five times with water to remove the magnesium sulfate. The resulting paste was then manually worked with a spatula on an FEP sheet to fibrillate the dispersed PTFE. The mass was then spread on a 1.75 cm diameter disk of approximately 0.5 mm thick conductive hydrophobic backing material (Electromedia Corp., Englewood, N.J.) by pressing at about 250 kg cm^{-2}. The electrodes were heat-treated at 330°C in flowing helium for 2 h in order to deactivate the Triton X-100 surfactant in the Teflon dispersion.

In order to obtain a reasonably porous electrode, it was found necessary to add ammonium bicarbonate as a pore-former. The initial method involved working the ammonium bicarbonate powder into the moist (with water) pyrochlore-Teflon paste. From 20 to 30 mg cm^{-2} was typically used (based on the electrode area). Much of the ammonium bicarbonate goes into solution in the moist paste and then reprecipitates as the paste dries.

A second method was instituted to avoid some of uncertainty as to the amount of pore-former that goes into solution in the moist paste. A slurry was prepared and mixed using a Waring-type blender with isopropanol, in which the ammonium bicarbonate is only slightly soluble. The slurry was then filtered, and then the resulting paste was worked, shaped and finally pressed, just as in the usual procedure.

E. Electrochemical Measurements

The gas-fed electrode measurements were carried out galvanostatically using a BC1200 Potentiostat (Stonehart Associates).

Each current was applied for a time sufficient to achieve steady state, usually 1-5 min. The IR drop was corrected using the current interruptor method, which corrects only for the solution resistance external to the porous electrode.

A diagrammatic sketch of the electrochemical cell used for high temperature experiments is shown in Fig. 2. An outer cylindrical shell of aluminum was heated with resistance heater elements, which were controlled with an Omega CN9000 microprocessor controller. The cell itself was made from Teflon, and a Viton O-ring sealed the cap to the main body. The cap assembly was bolted onto the bottom part of the aluminum shell. The working electrode shown in the diagram is of the flooded type for voltammetry and stability studies. For O_2 reduction measurements, a gas-fed electrode holder can be inserted, or alternatively, a floating electrode arrangement can be used. Hg/HgO reference electrodes employing either 5.5 M or 45 wt% (11.59 M) KOH were used for measurements at room temperature.For higher temperatures, where higher KOH concentrations existed, a dynamic hydrogen electrode was used.

IV. RESULTS AND DISCUSSION

A. Preparation and physical characterization of support materials and catalysts

A total of 43 different catalyst samples were prepared as part of this project (see Tables 1 and 2). These included mainly pyrochlores (22 samples) but also included RuO_2, both undoped and doped with

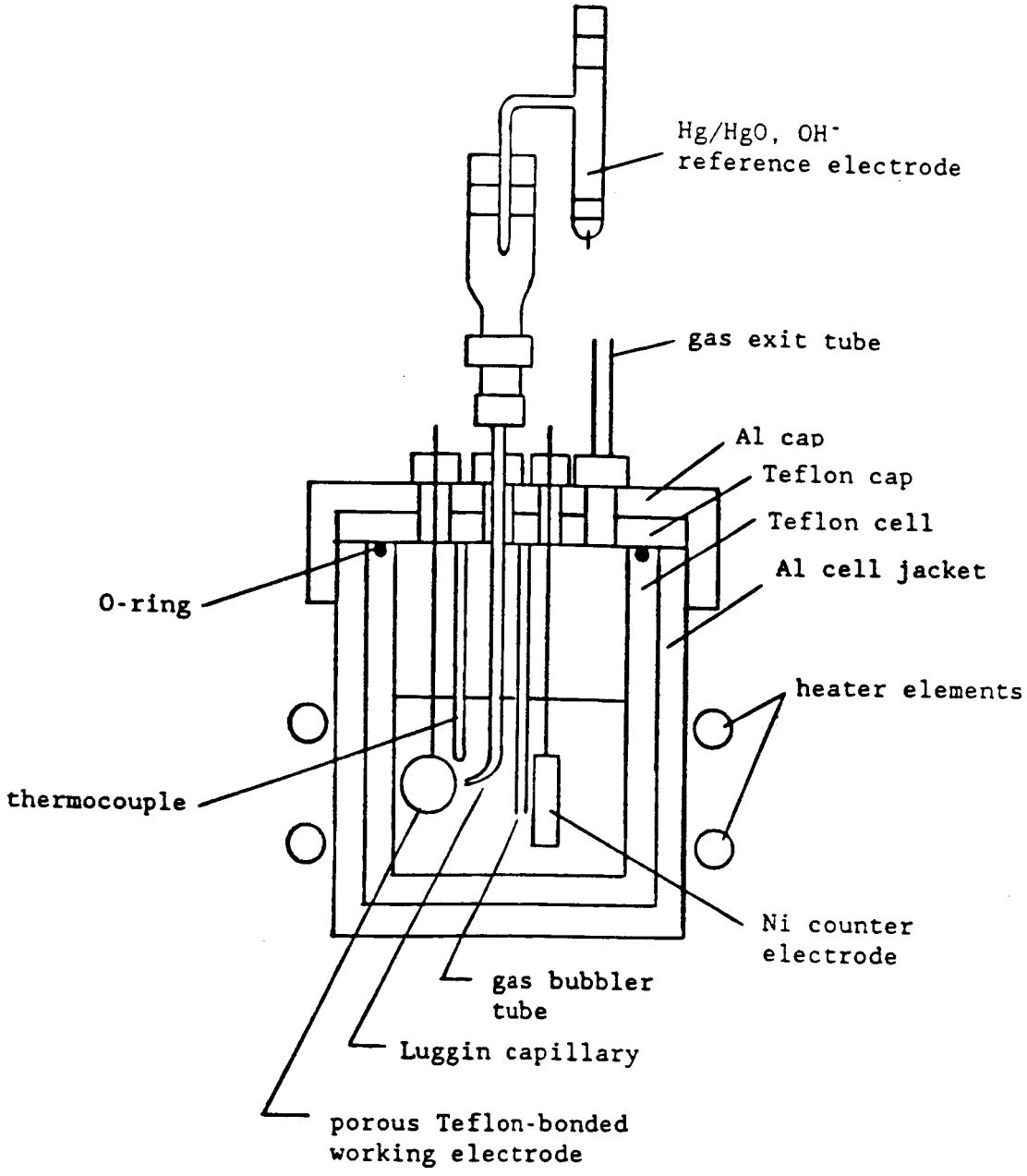

Fig. 2. Diagrammatic sketch of the electrochemical cell used for voltammetry and O_2 reduction polarization measurements at elevated temperatures ($\leq 220^{o}C$) in alkaline electrolyte.

platinum (6 samples). They were prepared mostly with the alkaline solution precipitation method (1-5) except for two that were prepared using the molten salt (fusion) technique (6-9). The latter has never been used, to our knowledge, to prepare pyrochlores. The XRD showed that this process successfully produced the pyrochlore. The BET surface area was not as high as expected (3.1 $m^2\ g^{-1}$), but it should be possible to improve this with better control of the processing variables.

The catalysts were characterized with X-ray diffraction (XRD) and BET surface area measurements, with some of the latter reaching quite high values (>100 $m^2\ g^{-1}$).

It should be noted that the Pb-Ir pyrochlore was found to be difficult to prepare in high area form, as was also found by Horowitz and coworkers (1). The product obtained using the alkaline solution method is typically amorphous and must be heat-treated to develop the crystallinity.

The conductivity for $Pb_2Ru_2O_{6.5}$ in the form of the high area powder was quite good [~170 $(\Omega\ cm)^{-1}$] when the powder was pressed to a density of 38% theoretical, which is in the range that might be used in the Teflon-bonded electrodes.

A series of Pt-doped lead ruthenate pyrochlores was prepared, and the X-ray diffraction (XRD) indicated that these materials retained the pyrochlore structure with no apparent additional phases. The use of the alkaline solution technique to prepare such compounds is new and was introduced as part of this project. These compounds were prepared with the idea of achieving atomic-level dispersion of the platinum in the pyrochlore, which could result in very high levels of catalytic activity if the Pt clusters are spaced far enough apart that the diffusion fields

around each cluster do not overlap. This so-called microelectrode effect has recently been described by Watanabe, Sei and Stonehart (see Ref. 15 and discussion below). With the pyrochlores that exhibit high activity for O_2 reduction, this effect will perhaps not be as pronounced as with supports that are not highly catalytic for O_2 reduction, such as RuO_2. It is interesting to compare the catalytic activity of these materials with that of Pt/pyrochlore samples prepared using more conventional methods, such as the Prototech method (12). One sample of the latter type was prepared.

The very high current density requirement means that the active catalyst layer should be kept as thin as possible to minimize the ohmic losses in the solution within the porous layer. The catalyst surface area must be as high as possible, however, to minimize the activation polarization.+

+ The catalytic activity per unit area appears to decrease with increasing area with highly dispersed platinum (16). This may occur because the higher index surfaces which become predominant with very small particles have smaller catalytic activity. Electronic factors may also be involved with small platinum clusters. Similar effects may occur with the gold-platinum and other bimetal clusters. Recently Watanabe et al. (15) have proposed that the apparent decrease in catalytic activity with highly dispersed platinum is not due to a crystallite effect but rather to interaction of the hemispherical O_2 concentration gradient around the nearest neighbor platinum particlesonthe substrate (Fig. 3). This effect depends on the distance between neighboring catalyst particles. The use of high area substrates should decrease the effect and lead to higher apparent catalytic activity.

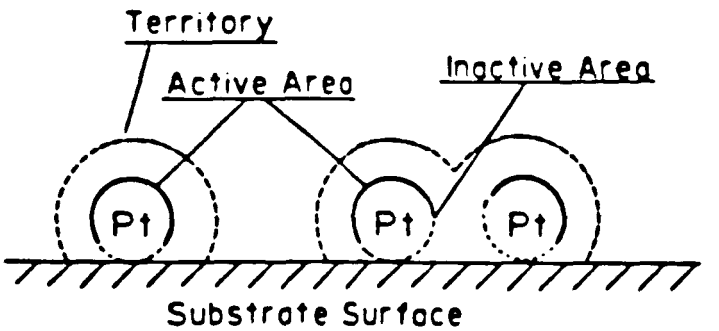

Fig. 3. Diagrammatic sketch of the interaction of the diffusion fields for an electroactive species such as O_2 around electrocatalyst particles on an inert (but electronically conductive) substrate (taken from Watanabe et al., Ref. 15).

To achieve both of these optimizations, the catalyst should be highly dispersed so as to obtain very high surface areas and at the same time be at high loadings to keep the active layer thin. This requires the use of high surface area supports. Modelling studies are required to establish what is the optimum support area and configuration, but areas of at least 50 $m^2\ g^{-1}$ probably are necessary for oxides consisting of predominantly the first transition row elements.

Conductivity measurements were carried out for a Pt-doped pyrochlore $Pb_2Ru_{1.8}Pt_{0.2}O_{7-y}$ as a function of theoretical density (Fig. 4). This compound showed lower conductivity than the undoped pyrochlore by ~25% at the highest density used. The conductivity of the undoped compound at this density (38% theoretical) is roughly a factor of 5 lower than that obtainable for powders pressed at higher pressures (13). Part of the difference may also be associated with the amorphous nature of this particular sample, which is known to lead to lower conductivity for this compound (13). The presence of platinum replacing part of the Ru in pyrochlores has been shown to lead to decreased conductivity in the Pb-Bi-Ru-Pt-O system (22). This is consistent with the fact that $Pb_2Pt_2O_7$ has relatively low conductivity (17), which is due to the filling of the t_{2g} conduction band (18). Lowered conductivity must be kept in mind as a possible problem with these types of catalysts.

In related work at CWRU, the temperature dependence of O_2 reduction on lithiated nickel oxide was examined. As a first step, powder samples were prepared, from which both porous as well as relatively-non-porous electrodes were made. These powders were also used in the NASA project as candidate support materials for noble metal

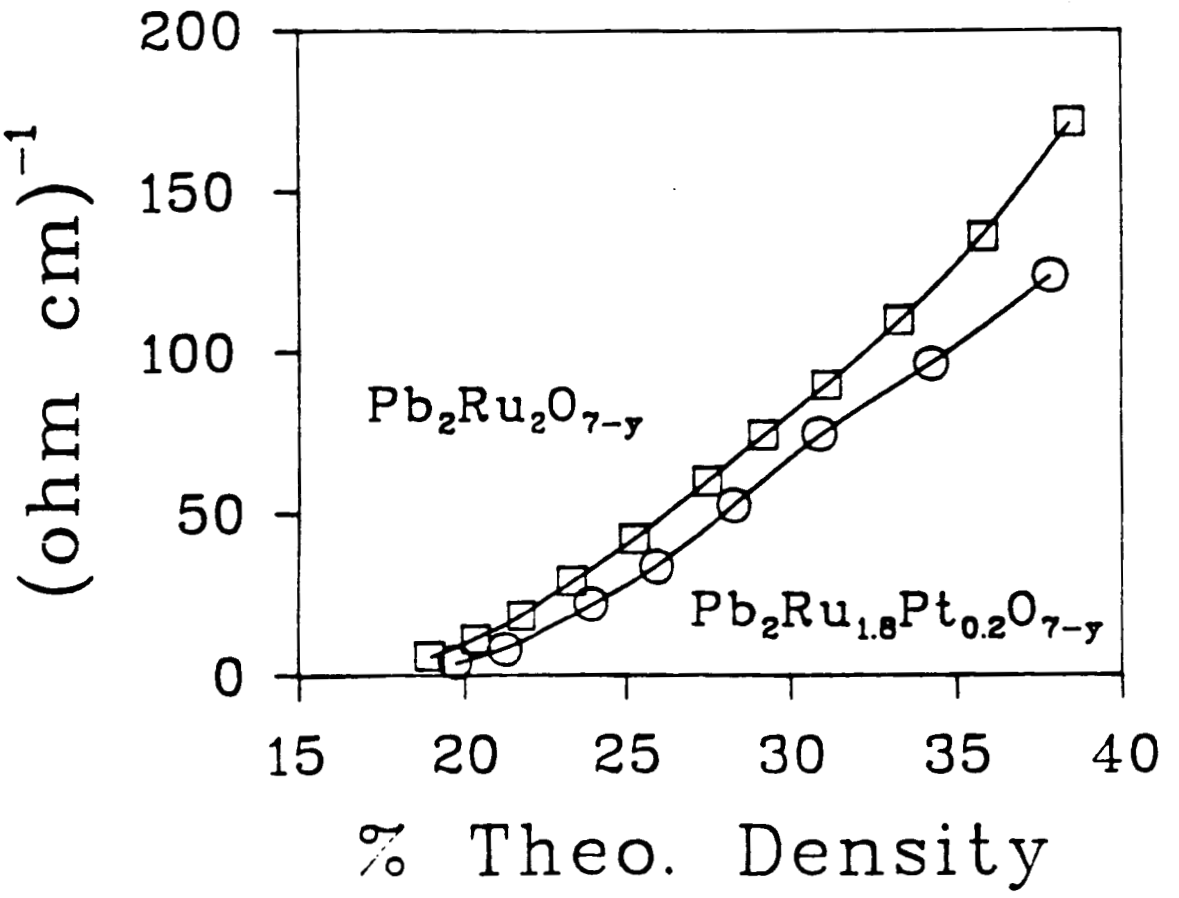

Fig. 4. Effect of Pt substitution in the $Pb_2Ru_2O_{7-y}$ pyrochlore on the conductivity at densities up to 38% theoretical using powder samples under pressure loads in the cell shown in Fig. 1.

catalysts. As mentioned earlier, $Ni_{0.9}Li_{0.1}O$ and $Ni_{0.96}Li_{0.04}O$ powders were prepared using a method involving the formation of an organic glass based on citric acid and urea. The powders were heat-treated in air at 650°C as well as higher temperatures and characterized using X-ray diffraction. The lattice parameters for the Li-NiO system are known to decrease with increasing amounts of Li doping (19, 20). Data from these two references are shown in Fig. 5 together with that for the compounds prepared at CWRU. The agreement with the literature data is rather good, but it should be pointed out that the Li content for the CWRU samples has not yet been confirmed analytically. These samples will be analyzed for Li content in the future using atomic emission spectroscopy. It was found that with higher heat treatment temperatures, e.g., 900 and 1200°C, substantial amounts of Li were lost from the sample. Evidence for this was an increase in the lattice parameter.

Discussions with Dr. Joseph Singer of NASA-Lewis have brought out the fact that the apparent lattice parameter for Li-NiO is somewhat dependent upon the preparation method. Tseung et al. (20) mention that the lattice parameter is highly sensitive to the presence of impurities. It could also be dependent upon heat treatment conditions such as the O_2 partial pressure, the time and the cooling rate. All of these factors can affect the concentration of cation vacancies, which could run as high as 1 at.%, which in turn affects the observed lattice parameter. Dr. Singer also pointed out that the lattice parameters obtained for Li-NiO samples prepared at high temperatures ($\geq$900°C) may not be valid for estimating Li content in samples prepared at lower temperatures. This will be checked in future work.

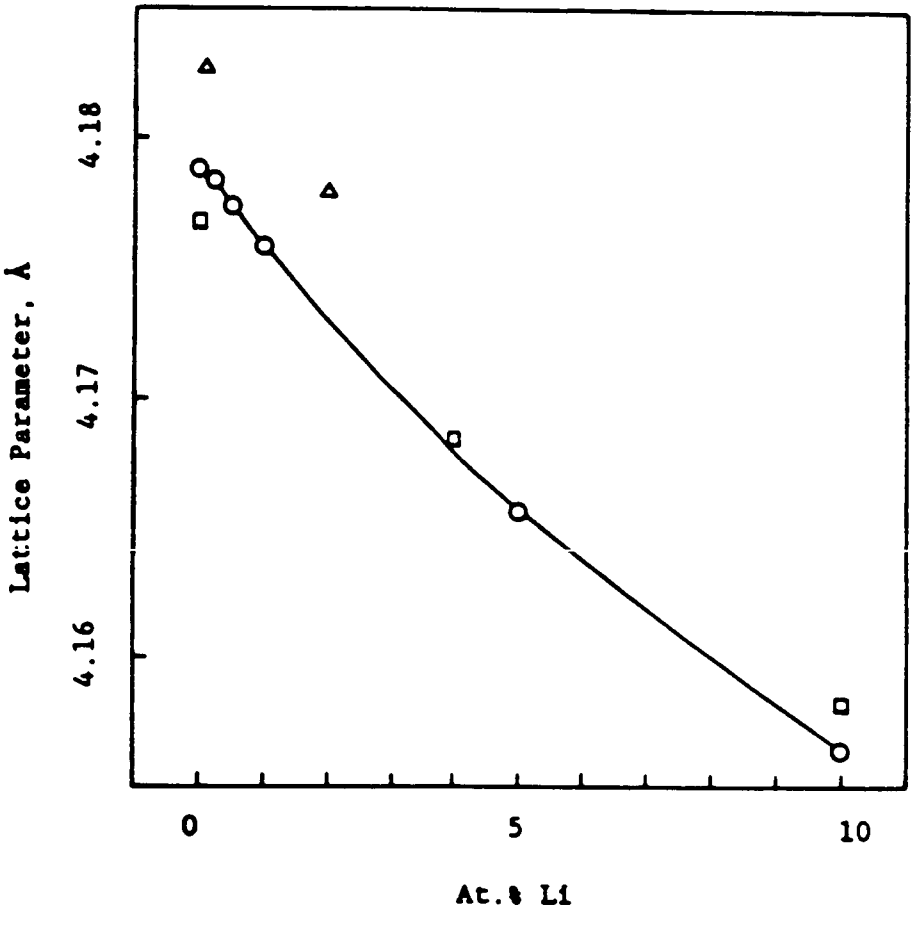

Fig. 5. Lattice parameters for lithium-doped nickel oxide: (o) data of Tseung et al. (20); (Δ) data of Verwey et al. (19); (□) present work, assuming that negligible lithium was lost when the samples were fired at 650°C for 24 h.

B. Electrochemical Characterization

After initial difficulties, the CWRU group had a good measure of success in the fabrication of pyrochlore-based gas-fed electrodes. Much of the experience in the fabrication of such electrodes at CWRU has involved structures based on high-area carbons. The fabrication methods must be modified significantly for structures not involving carbon, and the preferred method developed during this project made use of a pore-former material, ammonium bicarbonate. This was mixed with the pyrochlore-PTFE paste as discussed earlier, which yielded a pore structure with pores in the range of 1-2 μm, as seen by SEM (Fig. 6). The O_2 reduction polarization curves obtained for $Pb_2Ru_2O_{6.5}$-based electrodes in 5.5 M KOH at room temperature (Fig. 7) are among the best obtained in this laboratory for any catalyst, including the best transition metal macrocycles and platinum. Further electrode structure optimization could improve the high current density performance.

The incorporation of the pore-former into the "green" catalyst layer (before heat treatment at 320°C) was difficult to control in a reproducible fashion (Fig. 8). In some cases, the performance was as poor as that of electrodes fabricated without the benefit of a pore-former (Fig. 9). For this reason, the alcohol suspension method was initiated. Although more reproducible, it led to generally poorer performance (Fig. 10), due to the fact that very little porosity actually resulted at the 1 μm level, according to the SEM (Fig. 11b). A number of larger pores (10-20 μm) were observed (Fig. 11a). After the failure of this method, the methodology for reproducing the superior results of the wet paste method was optimized. This method can be

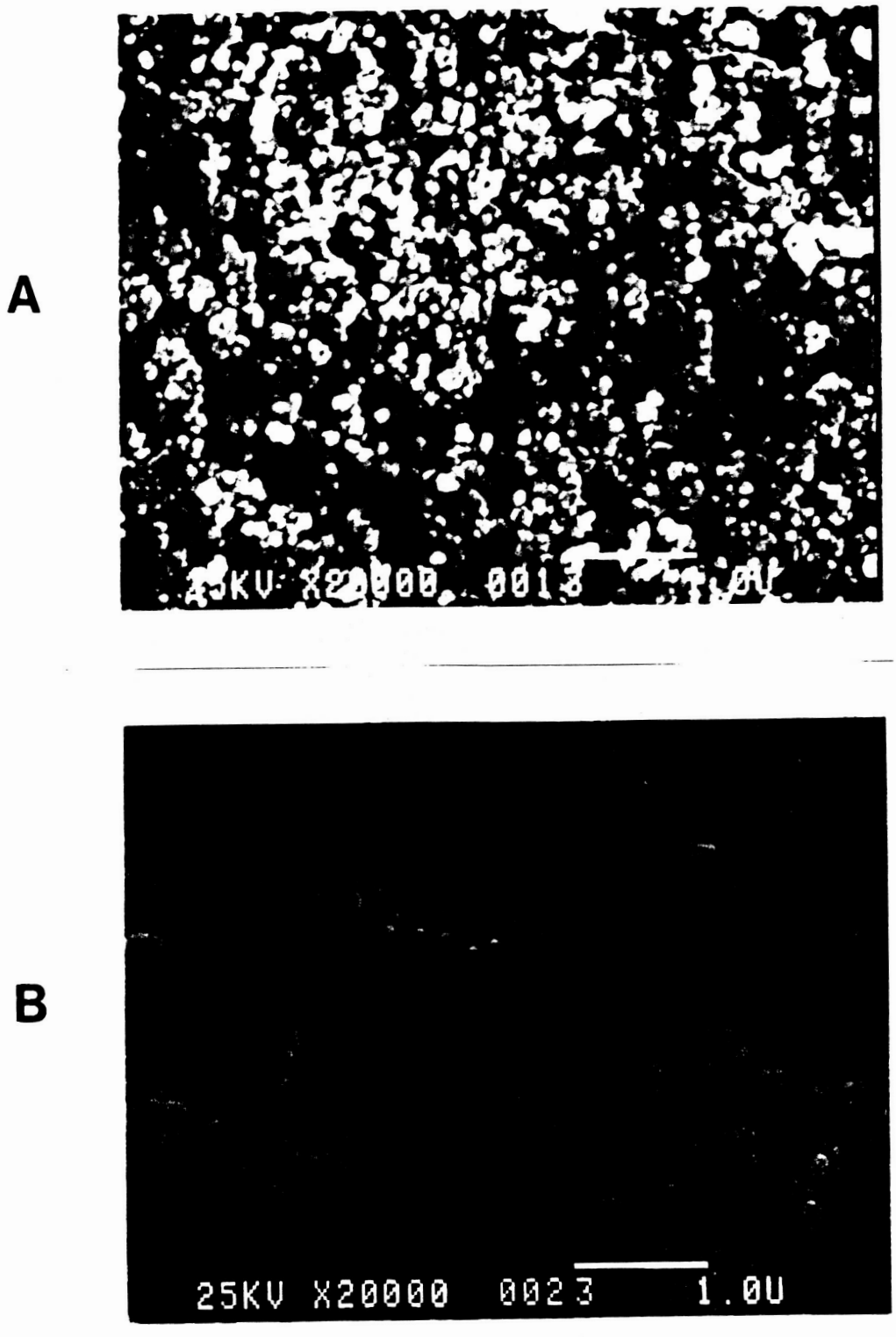

Fig. 6. Scanning electron micrographs of Teflon-bonded $Pb_2Ru_2O_{7-y}$ active layers fabricated A) without pore-former and B) with 9.6 mg cm^{-2} NH_4HCO_3 worked into the pyrochlore-Teflon paste while still moist. The electrodes contained 41.7 mg cm^{-2} pyrochlore and 13.9 mg cm^{-2} Teflon T30B. The electrodes had been subjected to polarization measurements on 10-6-89 (A) and 11-6-89 (B) respectively.

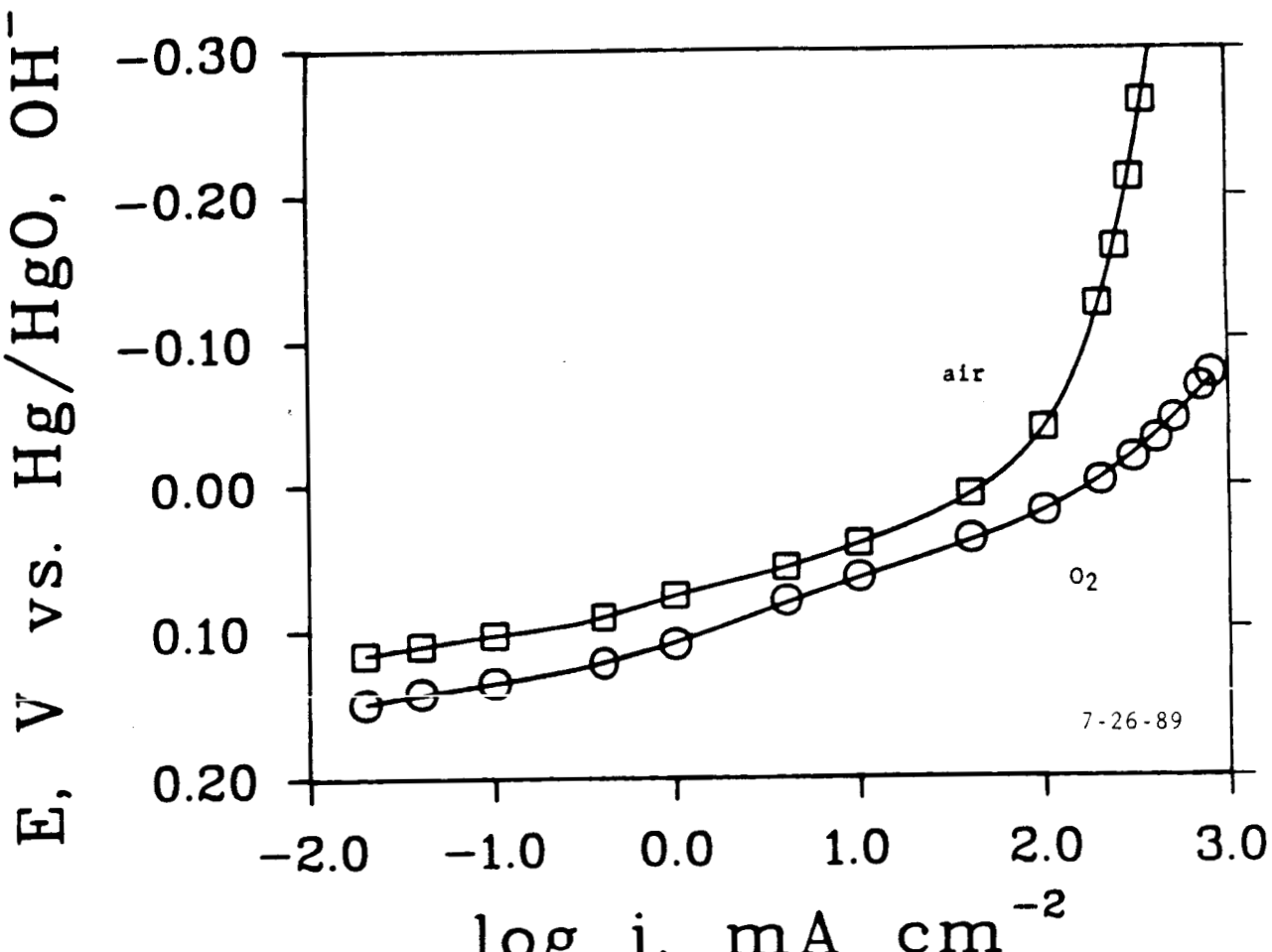

Fig. 7. Polarization curves for O_2 reduction with porous gas-fed (1 atm) electrodes in 5.5 M KOH at 25°C. The electrode contained 83.3 mg cm^{-2} pyrochlore and 27.8 mg cm^{-2} Teflon T30B and was heat-treated at 330°C for 2 h in flowing He. Ammonium bicarbonate (18.8 mg cm^{-2}) was added as a pore-former before the heat treatment.

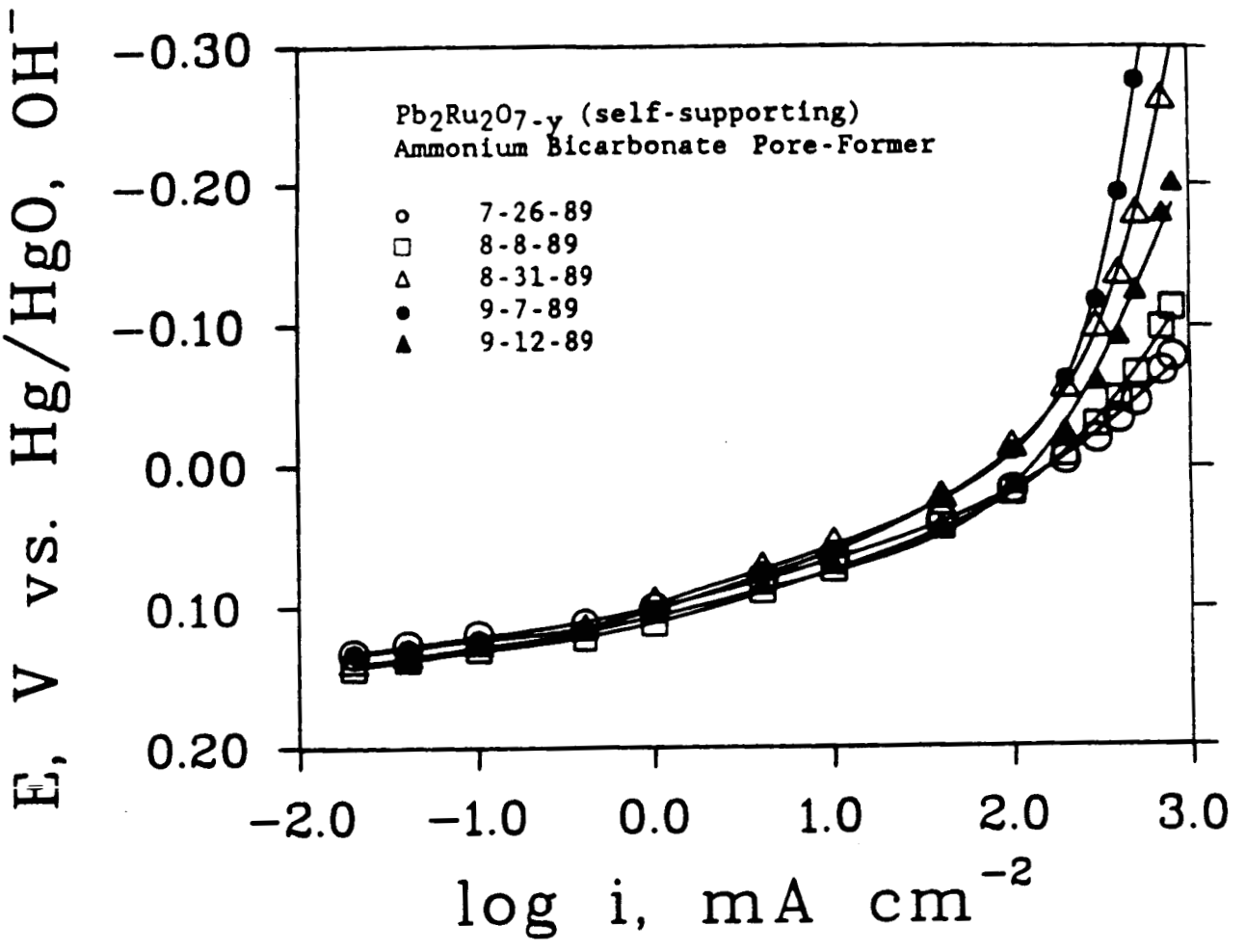

Fig. 8. Polarization curves for O_2 reduction with gas-fed electrodes using O_2 (1 atm) in 5.5 M KOH at 25°C. The electrodes contained 83.3 mg cm^{-2} pyrochlore and 27.8 mg cm^{-2} Teflon T30B. Ammonium bicarbonate (18.8 mg cm^{-2} for 7-26-89, 16.7 mg cm^{-2} for others) was worked into the moist pyrochlore- Teflon paste. The electrodes were heat-treated at 330°C for 2 h in flowing He. All of the curves were from the second polarization run and were recorded with decreasing current density.

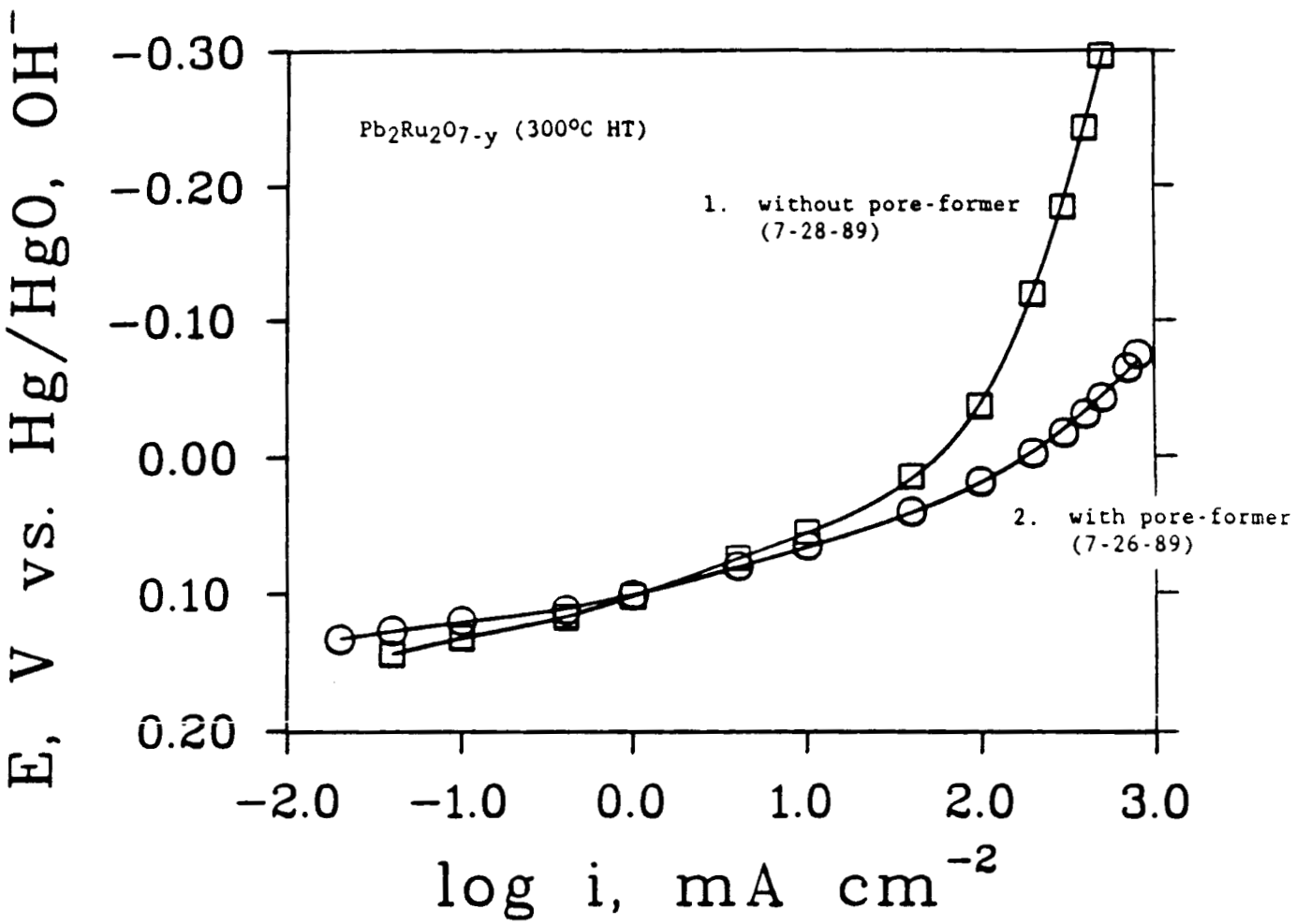

Fig. 9. Polarization curves for O_2 reduction with gas-fed electrodes using O_2 (1 atm) in 5.5 M KOH at 25°C. The electrodes contained 83.3 mg cm^{-2} pyrochlore and 27.8 mg cm^{-2} Teflon T30B. Ammonium bicarbonate (18.8 mg cm^{-2}) was used as a pore-former and was worked into the moist paste for the electrode in curve 2. The electrodes were heat-treated at 330°C for 2 h in flowing He.

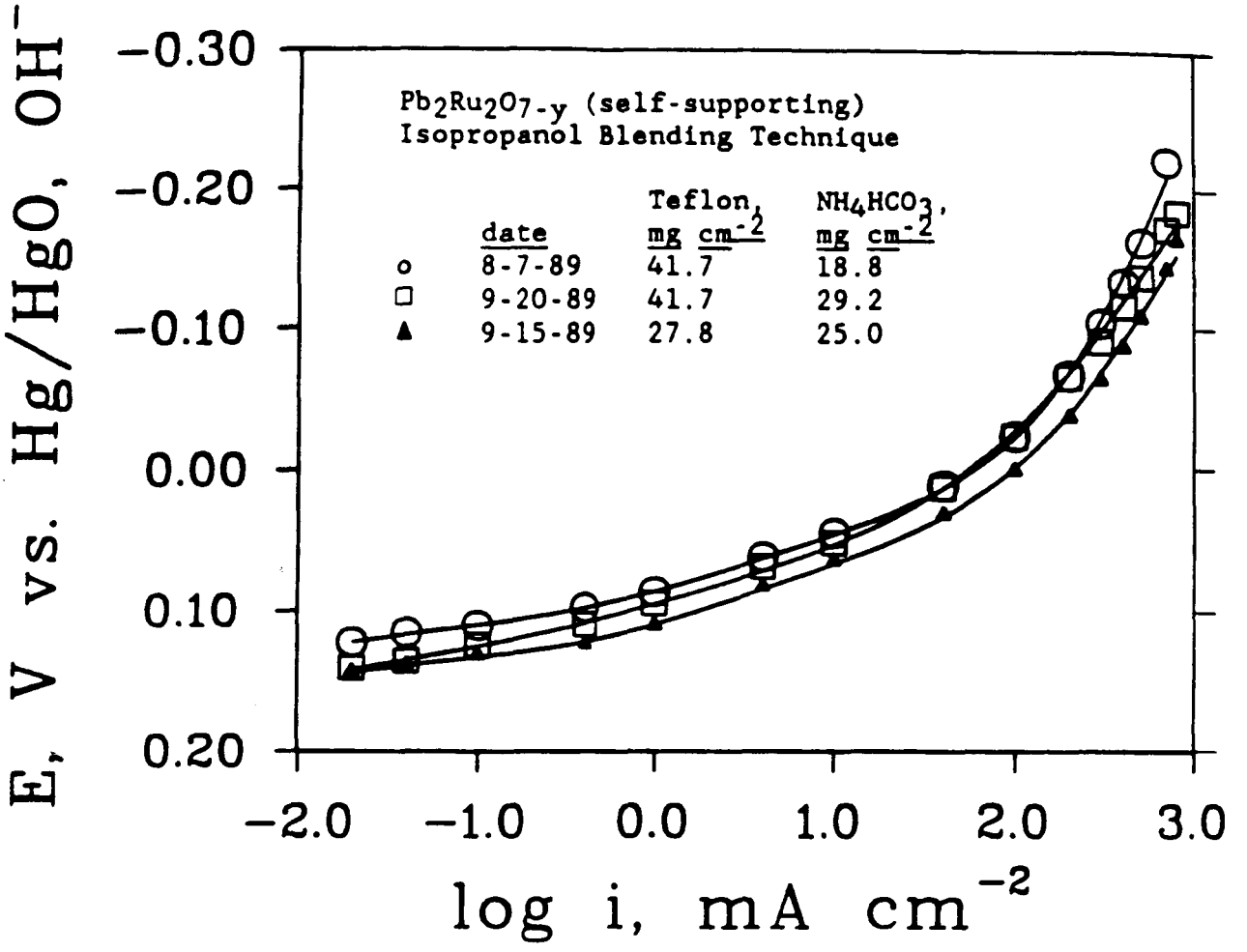

Fig. 10. Polarization curves for O_2 reduction with gas-fed electrodes using O_2 (1 atm) in 5.5 M KOH at 25 °C. The electrodes contained 83.3 mg cm^{-2} pyrochlore and designated amounts of Teflon T30B. Ammonium bicarbonate was used as a pore-former and was blended at high speed in a slurry in 2-propanol with the pyrochlore and Teflon. The electrodes were heat-treated at 330°C for 2 h in flowing He. All of the curves were from the first polarization run and were recorded with decreasing current density.

A

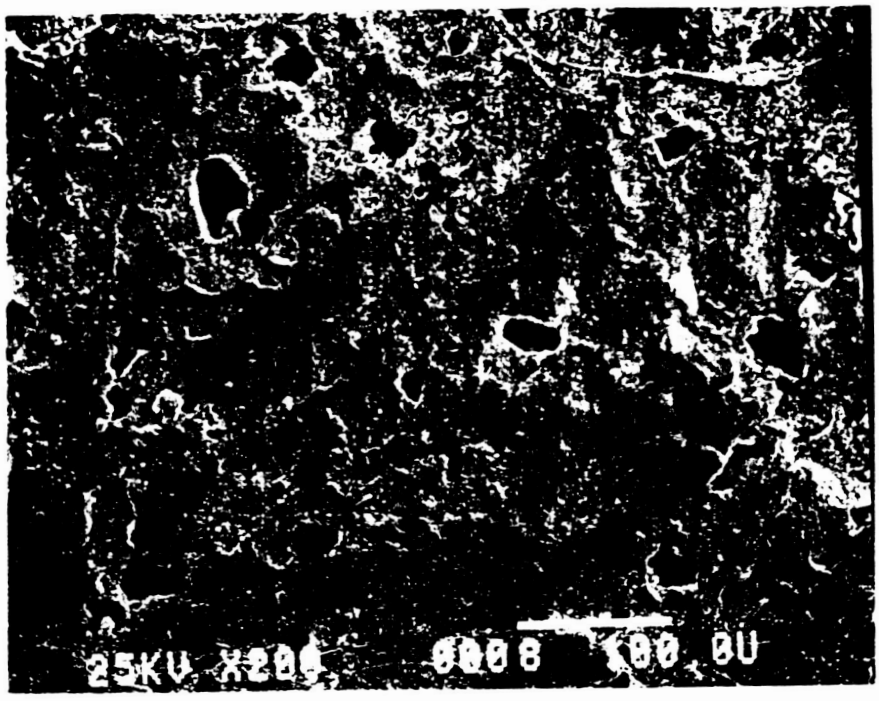

B

Fig. 11. Scanning electron micrographs of a Teflon-bonded $Pb_2Ru_2O_{7-y}$ active layer fabricated with 29.2 mg cm^{-2} NH_4CO_3 mixed with the pyrochlore (41.7 mg cm^{-2}) and Teflon (13.9 mg cm^{-2}) in an isopropanol slurry in a high-speed blender. The electrode had been subjected to polarization measurements on 9-20-89.

optimized further in future work in order to achieve better longer-term stability and high current density performance.

Preliminary examination of lead ruthenate was also carried out at higher temperatures (~140°C) in concentrated KOH in order to establish the stability under these conditions. Porous PTFE-bonded electrodes were fabricated on nickel screens and dipped in the electrolyte so that they became flooded. A nitrogen atmosphere was used. The voltammetry curves were obtained at a slow potential sweep rate so that the highly distributed impedance of the porous electrodes would be able to keep pace with the potential change (Fig. 12). These curves show that the electrodes were relatively stable over a period of at least several hours, and there was no sign of degradation at the end of the experiment. The three indicators of this stability were as follows:

1) The apparent capacitance, which is estimated from the vertical separation of the anodic and cathodic currents in relatively flat regions, did not change noticeably; this indicates that there was no loss of electrochemically active material. While this is not an extremely sensitive indicator, it would easily show a change of 5%.

2) There were only very slight changes in the shape of the voltammetry curves at potentials where there was apparently flow of Faradaic current, associated with either redox processes intrinsic to the oxide or O_2 generation, which would be expected at the more positive potentials. This indicated that there were no irreversible changes in the oxide over this potential region,

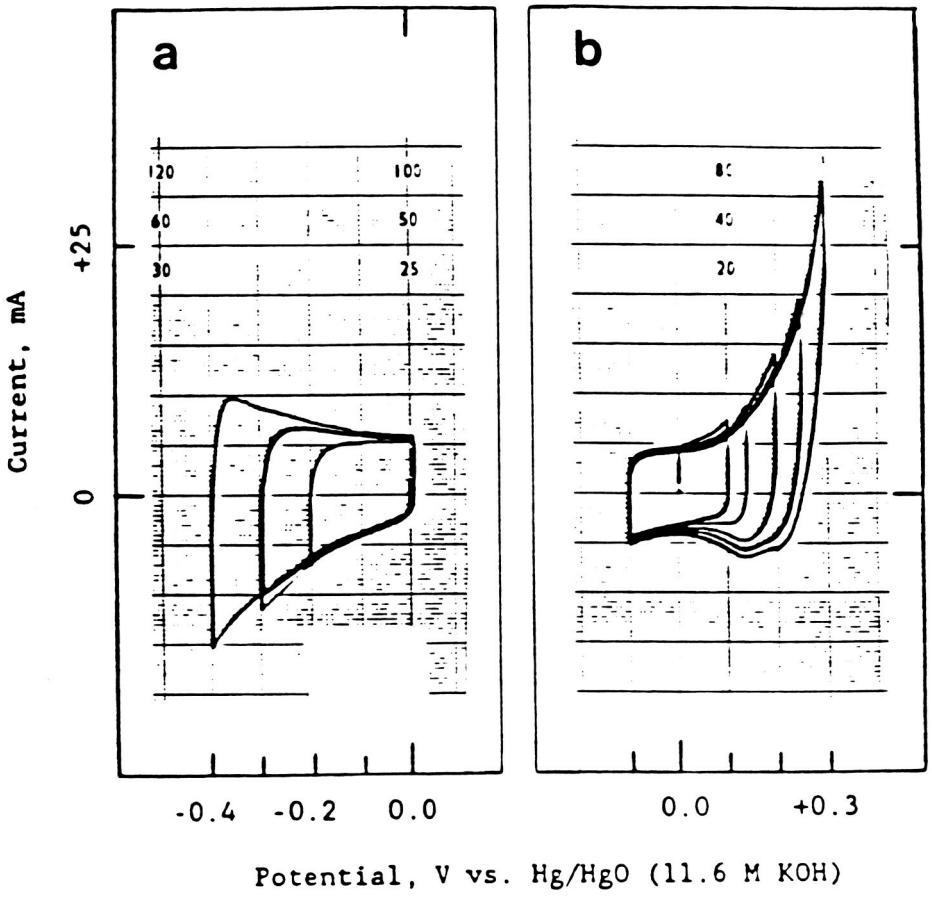

Fig. 12. Cyclic voltammetry curves in N_2-saturated 11.6 M KOH at 154 $\pm 2^{o}C$ for a PTFE-bonded porous electrode fabricated from $Pb_2Ru_2O_{7-y}$ (no heat treatment, 11.6 $m^2\ g^{-1}$ BET surface area; 41.7 mg cm^{-2} loading) and Teflon T30 (13.9 mg cm^{-2}): a) more negative potential range; b) more positive potential range. The electrode was heat-treated at 280°C for 3 h in flowing He.

which encompasses potentials which would commonly be experienced by an O_2 fuel cell cathode. Outside this region, irreversible changes are expected to occur based on present knowledge of the lead ruthenate.

3) When the potential sweep was reversed at intermediate points, there was a very reproducible steep rise or fall in the current. This indicates that there was good electronic conductivity within the electrode phase and that it did not degrade noticeably. The shapes of voltammetry curves at such reversal points have been mathematically modeled (21), and it is possible to estimate quantitatively the conductivity from the curves. Experience with other porous electrodes in this laboratory indicates that the behavior is similar to that of ones made from highly conductive carbon blacks.

The O_2 reduction behavior of such electrodes at elevated temperatures (~140°C) was also examined using the floating gas-fed electrode configuration (Fig. 13). The curve was similar to those obtained at room temperature (Fig. 10) for similar electrodes that were fabricated using the isopropanol blending technique. The polarization behavior was quite stable until the higher current densities were reached, where the performance began to degrade. Reasons for this degradation will be examined in future work.

Another indicator of the stability is the build-up of dissolved species in the electrolyte. This is a sensitive indicator in the case of ruthenium-containing compounds, because the orange $HRuO_4^-$ (ruthenate) ion is highly colored. In all of the experiments just described, there was a build-up of ruthenate, judging from the coloring of the

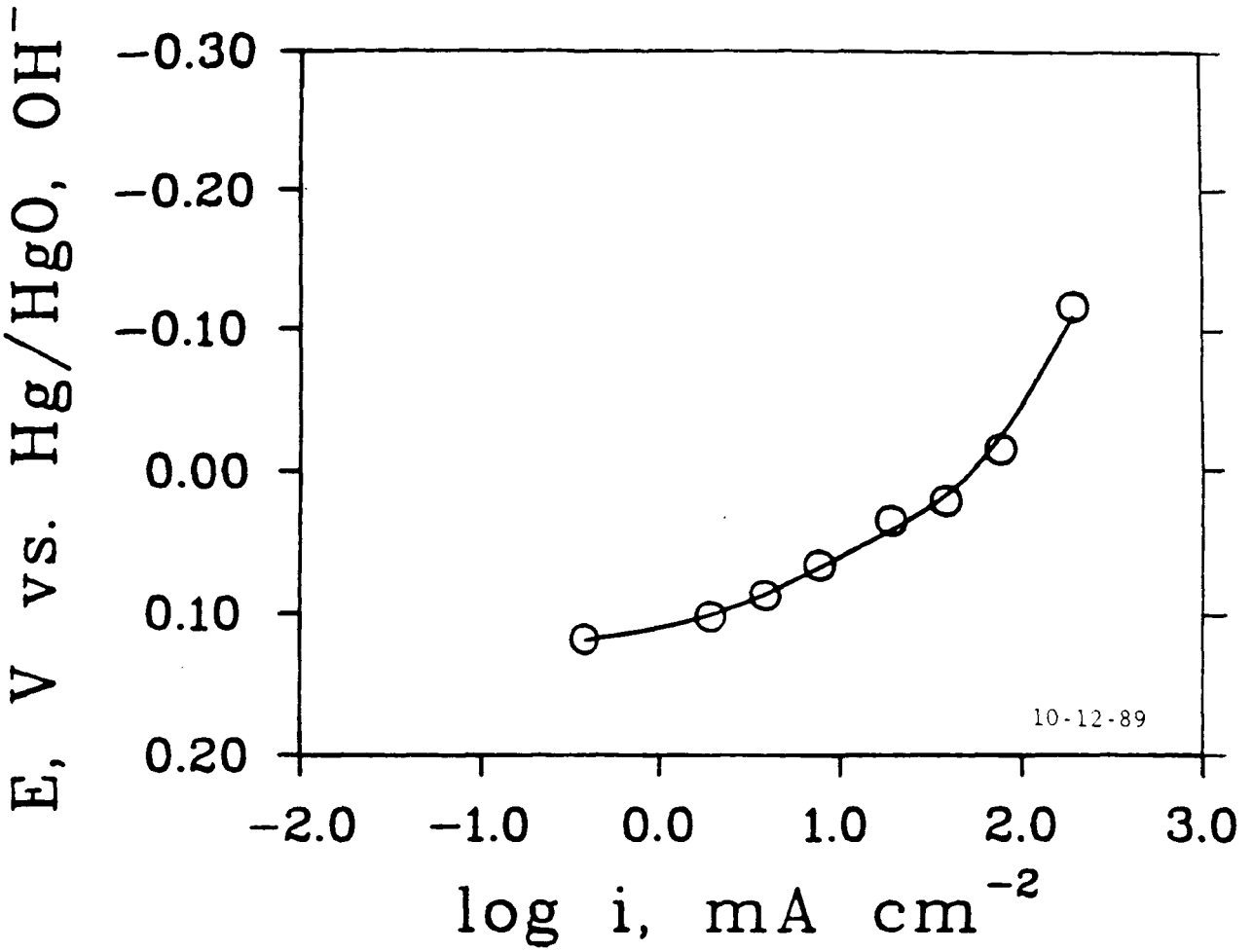

Fig. 13. Polarization curve for O_2 reduction for a gas-fed electrode using O_2 (1 atm) in 11.6 M KOH at 147.5°C. The PTFE-bonded electrode was fabricated with $Pb_2Ru_2O_{7-y}$ (heat-treated at 300°C in air for 24 h, 11.4 $m^2\ g^{-1}$ BET surface area, 41.7 mg cm^{-2} loading) and Teflon T30B (13.9 mg cm^{-2}). Ammonium bicarbonate (29.2 mg cm^{-2}) was used as a pore-former and was blended at high speed in 2-propanol with the pyrochlore and Teflon. The electrode was heat- treated at 330°C for 2 h in flowing He. Data were recorded point-by-point in the cathodic direction.

electrolyte. Future work will indicate whether this arises from dissolution of the pyrochlore or from traces of RuO_2, which are known to be present in some samples.

One way to stabilize the pyrochlore against dissolution is to place an anion-conducting membrane on the electrolyte side of the electrode. This impedes the diffusion of the metal oxy-anions, such as plumbate and ruthenate, out of the electrode. In a carbon-containing electrode with such a membrane (RAI type 4035, RAI Inc., Hauppage, NY), the performance and stability were significantly improved. The performance increased slowly over a ten-day period, reaching 90 mA cm^{-2} at 0.0 V vs. Hg/HgO. The performance showed no signs of decreasing when the measurements were terminated.

The CWRU group has developed several methods for modifying gas-fed electrodes with ion-conducting polymers, which could also be tried in future work with the pyrochlores. These methods have recently been patented (27).

It should be noted that the O_2 reduction results for $Pb_2Ru_2O_{6.5}$ described up to this point were obtained with a sample of relatively low area (11.4 m^2 g^{-1}) and good crystallinity (compound 1-6) prepared by Jai Prakash, a graduate student in Prof. Yeager's group. This compound was used for the electrode structure optimization because a large sample (~30 g) was available. Some of the higher area pyrochlores produced poor-quality electrodes when fabricated using the previously optimized method. This experience points out the need for electrode structure optimization of each individual sample.

In order to compare the O_2 reduction performance of some of the pyrochlores and other materials prepared for this project, it was found

to be expedient to prepare the gas-fed electrodes with roughly 50-50 wt% of acetylene black carbon. This procedure avoided the problem of optimizing fabrication conditions, because the fabrication of the carbon-based electrodes was apparently not affected significantly by the presence of the oxide. It can be seen from Table 3 that pyrochlore no. 1-13 was very similar in performance to pyrochlore 1-6. The current densities at 0.0 V vs. Hg/HgO (~0.93 V vs. RHE) were 10 and 20 mA cm^{-2} respectively. In an electrode based on pyrochlore 1-6 not containing carbon, the current density was 200 mA cm^{-2}, an order of magnitude higher than with carbon. This is only partly due to the fact that the electrode without carbon contained more of the pyrochlore (~40 vs. ~15 mg cm^{-2}). The explanation also involves the fact that the O_2 reduction process proceeds via the production of peroxide on the carbon, a process which occurs at a lower potential than the overall 4-electron reduction to hydroxide.

Experiments were carried out at higher temperatures using gas-fed electrodes fabricated from lithiated nickel oxide ($Ni_{0.9}Li_{0.1}O$). At temperatures approaching 200°C, the oxygen electrode reaction became essentially reversible, with negligible polarization at low current densities. At lower temperatures, e.g., 150°C, the electrocatalytic activity was much poorer. There is much interest in this result because of the insight it may provide into the kinetics and their dependence upon the surface electronic properties. Interestingly, only the lithiated NiO and platinized lithiated NiO showed significant improvements in performance with increased temperature.

Some O_2 reduction polarization results were obtained for platinum-containing catalysts. The Pt-doped lead ruthenate containing 4.75 at.%

Table 3: Selected O_2 Reduction Polarization Values for Oxide-based Electrocatalysts in Gas-Fed Electrodes at 25°C

comp. no.[a]	compound	BET[b] surf. area, $m^2 g^{-1}$	cd, mA cm^{-2} at 0.0 V[c]	date[d]
	Ru and Ir Compounds in Electrodes Containing Carbon			
1-06	$Pb_2Ru_2O_{7-y}$	11.4	20	03/09/89
1-06	$Pb_2Ru_2O_{7-y}$ + RAI membrane	11.4	90	03/20/89
1-29	$Ru_{0.98}Pt_{0.02}O_2$	68.1	1	01/18/90
1-17	$Pb_2Ru_2O_{7-y}$	3.5	5	01/19/90
1-24	$Pb_2Ru_{1.8}Pt_{0.2}O_{7-y}$	67.7	7	01/24/90
1-04	Pb-Ir oxide	66.0	8	01/26/90
1-10	$Pb_2Ru_2O_{7-y}$	104.6	5	01/30/90
1-13	$Pb_2Ru_2O_{7-y}$	66.1	10	01/31/90
	Platinized Nickel Oxide in Electrodes Containing Carbon			
2-07	$Ni_{0.9}Li_{0.1}O$ + 10 wt% Pt	0.86	3	10/17/89
2-07	$Ni_{0.9}Li_{0.1}O$ + 10 wt% Pt	0.86	15 (100°C)	10/25/89
	Ru Compounds in Electrodes not Containing Carbon			
1-06	$Pb_2Ru_2O_{7-y}$	11.4	200	07/26/89
1-19	$Pb_2Ru_{1.905}Pt_{0.095}O_{7-y}$	72.1	100	10/03/89
1-11	$Pb_2Ru_2O_{7-y}$	56.1	100	10/11/89
	Platinized Ru Compounds in Electrodes without Carbon			
1-05	$Pb_2Ru_2O_{7-y}$ + 10 wt% Pt	11.6	15	11/01/89
1-05	$Pb_2Ru_2O_{7-y}$ + 10 wt% Pt	11.6	70	11/03/89
	Nickel Oxide in Electrode without Carbon			
2-07	$Ni_{0.9}Li_{0.1}O$	0.86	3	10/12/89
	Platinized Nickel Oxide in Electrode without Carbon			
2-07	$Ni_{0.9}Li_{0.1}O$	0.86	25	10/18/89

a. The compound number refers to the table number (1 or 2) followed by the listing number in the table.
b. The BET surface areas are for the oxides themselves, even in cases where the oxides were platinized.
c. Current density at 0.0 V vs. Hg/HgO, OH^- in 5.5 M KOH at 25°C with 1 atm O_2.
d. Date of the polarization measurement.

Pt (compound 1-19) showed only a slight improvement in O_2 reduction performance at the higher current densities as compared with the undoped material, although surprisingly the potentials reached at low current density were as high as +0.208 V vs. Hg/HgO, OH^- (Fig. 14). The similarity at high cd may be due to several factors:

1) the electronic conductivity of Pt-rich phases may be poor, as discussed earlier;
2) the catalytic activity of the Pt may be only slightly higher that of the pyrochlore itself;
3) the Pt may not have become fully incorporated into the structure, i.e., it may be agglomerated; or
4) the Pt may not be present in the same level it was added, i.e., there may have been some loss.

These possibilities will be examined in future work.

It was observed that samples of $Pb_2Ru_2O_{7-y}$ that were amorphous had very poor stability in the KOH electrolyte even at 25°C. This may be understandable in the light of the electrochemical behavior of the pyrochlore vs. that of other ruthenium oxides. It is known that hydrated RuO_2 can be oxidized to the +6 oxidation state, which can readily yield the soluble ruthenate ion at potentials in the +0.4 V vs. Hg/HgO range (23), whereas it appears that the pyrochlore does not go to Ru^{6+} until the potential is positive of +0.5 V vs. Hg/HgO (24, 25). Thus the crystalline pyrochlore should be more stable than the amorphous forms. The amorphous $Pb_2Ir_2O_{7-y}$ was also found to be unstable at the more positive potentials.

The $Ni_{0.9}Li_{0.1}O$ with deposited Pt yielded a much enhanced performance for O_2 reduction at 25°C compared to the unadorned oxide in

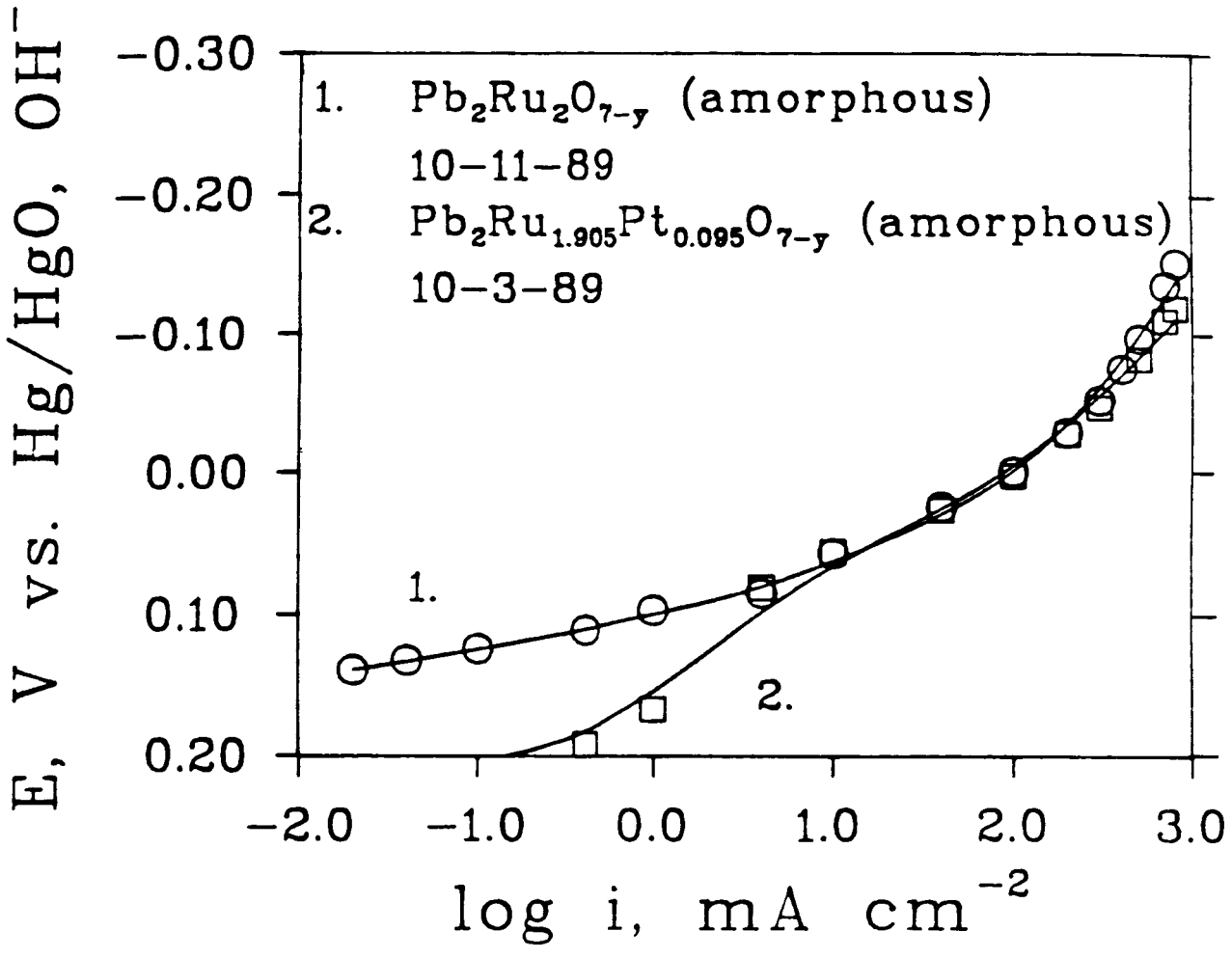

Fig. 14. Polarization curves for O_2 reduction with gas-fed electrodes using O_2 (1 atm) in 5.5 M KOH at 25°C. The electrodes contained 41.7 mg cm^{-2} oxide and 13.9 mg cm^{-2} Teflon T30B. Ammonium bicarbonate (18.8 mg cm^{-2}) was used as a pore-former and was blended at high speed in a slurry in 2-propanol with the oxides and Teflon. The electrodes were heat-treated at 320°C for 2 h in flowing He.

electrodes not containing carbon (Fig. 15). The current density at 0.0 V vs. Hg/HgO was 25 mA cm^{-2}, which is relatively low. This was probably due to the very low area of the material (< 1 m^2 g^{-1}). Also, the current density would be expected to be much higher at elevated temperatures. For example, the current density increased by a factor of 5 with an increase in temperature form 25 to 100°C for a Pt-Li-NiO electrode containing carbon (Table 3).

The lithiated NiO was also deposited with gold, but the O_2 reduction performance was much poorer than for the unadorned oxide (Fig. 16). This may have been due to a modification of the oxide (e.g., reduction) during the deposition process. In the same figure, the performance for the platinized Li-NiO on air was good. In pure O_2, the performance would be expected to be as much as a factor of 5 higher in a well-optimized electrode.

V. SUMMARY OF RESULTS AND CONCLUSIONS

1. The alkaline solution technique was successful in preparing the stoichiometric $Pb_2Ru_2O_{7-y}$ in relatively high area form, in one case over 100 m^2 g^{-1}, confirming the result of Horowitz et al.;
2. The alkaline solution technique was also successful in preparing Pt-doped Pb-Ru pyrochlores with high areas for the first time;
3. The molten salt technique was successful in preparing the Pb-Ru pyrochlore for the first time;
4. RuO_2 and Pt-doped RuO_2 were prepared using the citric acid-urea method for the first time;

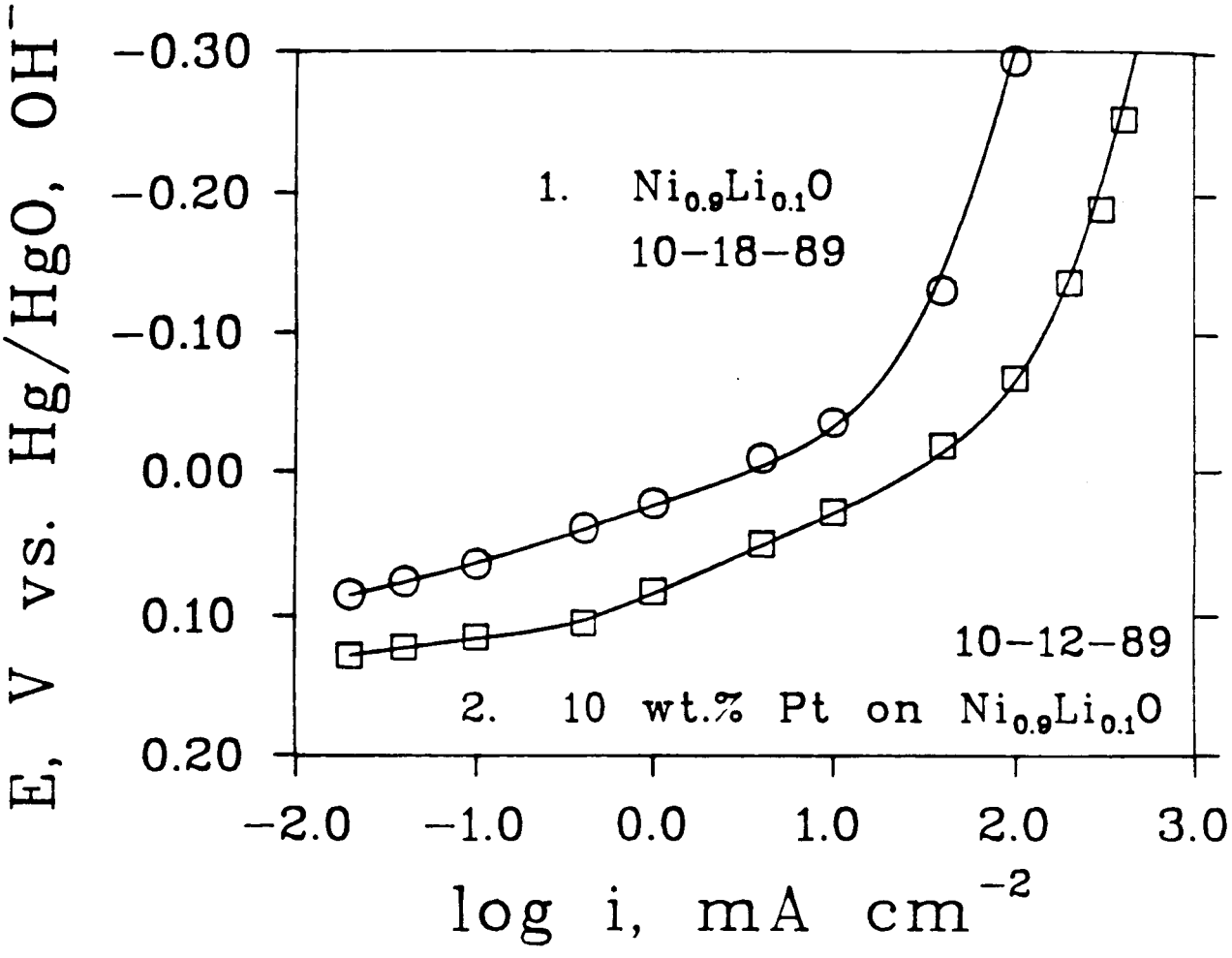

Fig. 15. Polarization curves for O_2 reduction with gas-fed electrodes using O_2 (1 atm) in 5.5 M KOH at 25°C. The electrodes contained 41.7 mg cm^{-2} oxide and 8.5 mg cm^{-2} Teflon T30B. Ammonium bicarbonate (12.5 mg cm^{-2}) was used as a pore-former and was blended at high speed in a slurry in 2-propanol with the oxides and Teflon. The electrodes were heat-treated at 320°C for 2 h in flowing He.

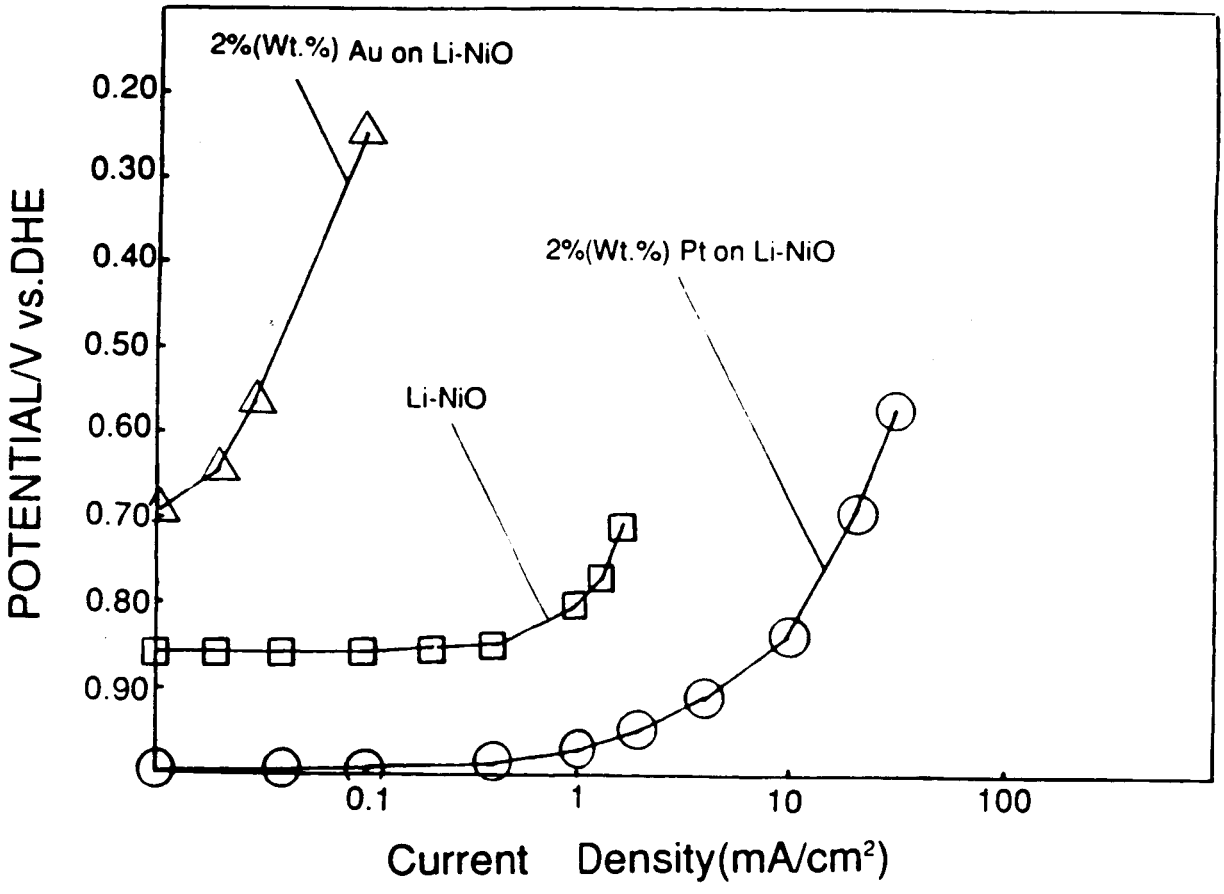

Fig. 16. Polarization curves for O_2 reduction in 11.7 M KOH at 147°C. Electrodes contained 41.7 mg cm^{-2} lithiated NiO and 13.9 mg cm^{-2} Teflon T30B. The lithiated NiO powder had a BET surface area of2.56 m^2 g^{-1}. Data were recorded point-by-point in the cathodic direction using 1 atm air.

5. Lithiated nickel oxides were prepared using the citric acid-urea method for the first time, although the areas were low;
6. $Pb_2Ru_2O_{7-y}$ was fabricated into self-supporting PTFE-bonded O_2 electrodes with very high performance for O_2 reduction at room temperature;
7. An anion-conducting membrane increased the performance and stability of a carbon-based $Pb_2Ru_2O_{7-y}$ electrode
8. $Pb_2Ru_2O_{7-y}$ was found to be relatively stable over the potential range relevant for the O_2 cathode at ~140°C in concentrated KOH.
9. The O_2 reduction performance for $Pb_2Ru_2O_{7-y}$ was encouraging and relatively stable even in a non-optimized electrode at ~140°C.
10. The electrode fabrication technique for electrodes not containing carbon could not be optimized for many of the materials given the time and quantity available.
11. Amorphous materials prepared as $Pb_2Ru_2O_{7-y}$ and also $Pb_2Ir_2O_{7-y}$ were relatively unstable in solution at room temperature.
12. The $Ni_{0.9}Li_{0.1}O$ yielded nearly reversible behavior for the O_2/OH^- redox couple at temperatures approaching 200°C over a substantial current density range.
13. The Pt-doped $Pb_2Ru_2O_{7-y}$ produced only a slight improvement in O_2 reduction performance, for several possible reasons.
14. Pt deposited on $Ni_{0.9}Li_{0.1}O$ yielded a very substantial improvement in O_2 reduction performance even though the support was in low area form.
15. Au deposited on Li-NiO yielded very poor O_2 reduction performance.

VI REFERENCES

1. H. S. Horowitz, J. M. Longo and J. T. Lewandowski, U. S. Patent 4,129,525, December 12, 1978.
2. H. S. Horowitz, J. M. Longo and J. T. Lewandowski, U. S. Patent 4,176,094, November 27, 1979.
3. H. S. Horowitz, J. M. Longo and J. T. Lewandowski, U. S. Patent 4,203,871, May 20, 1980.
4. H. S. Horowitz, J. M. Longo and J. T. Lewandowski, Mat. Res. Bull., 16, 489 (1981).
5. H. S. Horowitz, J. M. Longo, H. H. Horowitz and J. T. Lewandowski, in "Solid State Chemistry in Catalysis," ACS Symposium Series 279, R. K. Grasselli and J. F. Brazdil, Editors, pp. 143-163, American Chemical Society, Washington, D. C. (1985).
6. R. H. Arendt and M. J. Curran, J. Electrochem. Soc., 127, 1660 (1980).
7. R. H. Arendt, ibid., 129, 979 (1982).
8. C. E. Baumgartner, R. H. Arendt, C. D. Iacovangelo and B. R. Karas, ibid., 131, 2217 (1984).
9. E. N. Balko and C. R. Davidson, J. Inorg. Nucl. Chem., 42, 1778 (1980).
10. C. C. Chen and H. U. Anderson, University of Missouri-Rolla, preprint.
11. M. S. G. Baythoun and F. R. Sale, J. Mat. Science, 17, 2757 (1982).
12. see for example, H. G. Petrow and R. J. Allen, U. S. Patent 3,992,331, November 16, 1976.

13. R. A. Beyerlein, H. S. Horowitz and J. M. Longo, Solid State Chem., 72, 2 (1988).

14. E. Espinola, P. M. Miguel, M. R. Salles and A. R. Pinto, Carbon, 24, 337 (1986).

15. M. Watanabe, H. Sei and P. Stonehart, J. Electroanal. Chem., 261, 375 (1989).

16. K. Kinoshita, J. Electrochem. Soc., 137, 845 (1990).

17. A. W. Sleight, Mat. Res. Bull., 6, 775 (1971).

18. V. B. Lazarev and I. S. Shlaplygin, Mat. Res. Bull., 13, 229 (1978).

19. E. J. W. Verwey, P. W. Haaijman, F. C. Romeijn and G. W. van Oosterhout, Philips Res. Rep., 5, 173 (1950).

20. A. C. C. Tseung, B. S. Hobbs and A. D. S. Tantram, Electrochim. Acta., 15, 473 (1970). 21. L. G. Austin and E. G. Gagnon, J. Electrochem. Soc., 120, 251 (1973).

22. G. Mayer-von Kürthy, W. Wishert, R. Kiemel, S. Kemmler-Sack, R. Gross and R. P. Huebner, J. Solid State Chem., 79, 34 (1989).

23. L. D. Burke and O. J. Murphy, J. Electroanal. Chem., 109, 199 (1980).

24. J. B. Goodenough, R. Manoharan and M. Paranthaman, J. Am. Chem. Soc., 112, 2076 (1990).

25. J. Prakash, D. Tryk and E. Yeager, J. Power Sources, 29, 413 (1990)

26. L Swette and N. Kackley, paper presented at the Space Electrochemical Research and Technology Conference, April 9-10, 1991, NASA Lewis Research Center, Cleveland, Ohio.

27. A. Z. Gordon, E. B. Yeager, D. A. Tryk and M. S. Hossain, International Patent Application Numbers WO88/06642, 06643, 06644, 06645, 06646 and 08888, September 7, 1988.

Appendix 1
Further Experimental Information
on Ruthenium and Iridium-Based Transition Metal Oxides Prepared for this Project

Compound	date prep.	latt. param. a_0, Å	prep. cond.[a] pH	temp., °C	time, h	O_2[a]	salts used[a]
Pb-Ir compounds							
1. $Pb_2Ir_2O_{7-y}$	05/10/89	-	>14	65	?	Y	Pb ac, Ir Cl
2. $Pb_2Ir_2O_{7-y}$	05/10/89	-	>14	65	?	Y	Pb ac, Ir Cl
3. Pb-Ir oxide	08/15/89	-	13	65	8	Y	Pb ac, Ir Cl
4. Pb-Ir oxide	08/15/89	-	13	65	8	Y	Pb ac, Ir Cl
Pb-Ru compounds							
5. $Pb_2Ru_2O_{7-y}$	03/03/89	-	>14	75	48	Y	Pb ac, Ru Cl
6. $Pb_2Ru_2O_{7-y}$	03/03/89	-	>14	75	48	Y	Pb ac, Ru Cl
7. $Pb_2Ru_2O_{7-y}$	05/10/89	-	>14	65	?	Y	Pb ac, Ru Cl
8. $Pb_2Ru_2O_{7-y}$	05/10/89	-	>14	65	?	Y	Pb ac, Ru Cl
9. $Pb_2Ru_2O_{7-y}$	06/13/89	-	NA	525	4	NA	Pb ac, Ru Cl
10. $Pb_2Ru_2O_{7-y}$	08/15/89	-	13	65	8	Y	Pb ac, Ru Cl
11. $Pb_2Ru_2O_{7-y}$	08/15/89	-	13	65	8	Y	Pb ac, Ru Cl
12. $Pb_2Ru_2O_{7-y}$	10/09/89	-	12	72	1.8	N	Pb ac, Ru Cl
13. $Pb_2Ru_2O_{7-y}$	10/09/89	-	12	72	1.8	Y	Pb ac, Ru Cl
14. $Pb_2Ru_2O_{7-y}$	10/09/89	-	12	25	1.8	Y	Pb ac, Ru Cl
15. $Pb_2Ru_2O_{7-y}$	10/09/89	-	12	25	1.8	N	Pb ac, Ru Cl
16. $Pb_2Ru_2O_{7-y}$	10/25/89	10.348	?	67	2.5	Y	Pb ac, Ru Cl
17. $Pb_2Ru_2O_{7-y}$	11/29/89	10.287	?	25	16	N?	Pb ac, Ru Cl
Pb-Ru-Pt compounds							
18. $Pb_2Ru_{1.98}Pt_{.02}O_{7-y}$	09/05/89	-	12.2	65	3	Y	Pb ac, Ru, Pt Cl
19. $Pb_2Ru_{1.905}Pt_{.095}O_{7-y}$	09/08/89	-	12.2	55	3	Y	Pb ac, Ru, Pt Cl
20. $Pb_2Ru_{1.98}Pt_{0.02}O_{7-y}$	10/19/89	10.373	?	67	2.5	Y	Pb ac, Ru, Pt Cl
21. $Pb_2Ru_{1.9}Pt_{.1}O_{7-y}$	11/02/89	10.364	?	75	2.2	Y	Pb ac, Ru, Pt Cl
22. $Pb_2Ru_{1.8}Pt_{.2}O_{7-y}$	11/02/89	10.384	?	75	2.2	Y	Pb ac, Ru, Pt Cl
23. $Pb_2Ru_{1.98}Pt_{.02}O_{7-y}$	11/29/89	10.284	?	25	16	N	Pb ac, Ru, Pt Cl
24. $Pb_2Ru_{1.94}Pt_{.06}O_{7-y}$	11/29/89	10.284	?	25	16	N	Pb ac, Ru, Pt Cl

(continued on next page)

Appendix 1 (continued)
Further Experimental Information
on Ruthenium and Iridium-Based Transition Metal Oxides Prepared for this Project

Compound	date prep.	latt. param. a_0, Å	prep. cond.[a] pH	temp., °C	time, h	O_2[a]	salts used[a]
25. $Pb_2Ru_{1.9}Pt_{0.1}O_{7-y}$	11/29/89	10.284	?	25	16	N	Pb ac, Ru, Pt Cl
<u>RuO_2-based compounds</u>							
26. RuO_2	06/13/89	-	NA	500	3	NA	Pb ac, Ru Cl
27. RuO_2	06/13/89	-	NA	500	3	NA	Pb ac, Ru Cl
28. RuO_2	09/08/89	-	10.5	45	2	N	Ru Cl
29. $Ru_{.98}Pt_{.02}O_2$	09/08/89	-	10.5	45	2	N	Ru, Pt Cl
30. $Ru_{.9}Pt_{.1}O_2$	11/22/89	-	NA	NA	NA	NA	Ru, Pt Cl
31. $Ru_{.5}Pt_{.5}O_2$	11/22/89	-	NA	NA	NA	NA	Ru, Pt Cl
<u>Ru-containing perovskites</u>							
32. $SrRuO_3$	05/10/89	-	13	25	?	N	Sr NO_3^-, Ru Cl
33. $CaRuO_3$	05/10/89	-	13	25	?	N	Ca ac, Ru Cl

a. abbreviations: ac = acetate; NA = not applicable
b. O_2 indicates oxygen bubbling during the alkaline solution reaction.

Appendix 2
Further Experimental Information
on Nickel-Based Oxides Prepared for this Project

Compound	date prep.	latt. param. a_0, Å	resist. Ω cm[a]	salts, compounds used[b]
Nickel Oxide-Based Compounds				
1. NiO	09/08/89	-	-	Ni ac, Li carb, CA, ED
2. $Ni_{0.98}Li_{0.02}O$	09/08/89	-	-	Ni ac, Li carb, CA, ED
3. $Ni_{0.96}Li_{0.04}O$	09/08/89	-	-	Ni ac, Li carb, CA, ED
4. $Ni_{0.94}Li_{0.06}O$	09/08/89	-	-	Ni ac, Li carb, CA, ED
5. NiO	09/22/89	4.177	-	Ni ac, Li carb, CA, urea
6. $Ni_{0.96}Li_{0.04}O$	09/22/89	4.169	-	Ni ac, Li carb, CA, urea
7. $Ni_{0.9}Li_{0.1}O$	09/22/89	4.159	-	Ni ac, Li carb, CA, urea
8. $Ni_{0.95}Li_{0.05}O$	10/02/90	-	-	Ni nit, Li nit, CA, ED
9. $Ni_{0.95}Li_{0.05}O$	10/02/90	-	-	Ni nit, Li nit, CA, ED
10. $Ni_{>0.99}Li_{<0.01}O$	10/03/90	-	$1x10^5$	Ni nit, Li ac, NaOH
11. $Ni_{0.98}Li_{0.02}O$	11/09/90	-	-	Ni ac, Li ac
12. $Ni_{>0.99}Li_{<0.01}O$	11/14/90	-	$5x10^5$	Ni nit, Li ac, Na_2CO_3
13. $Ni_{0.9}Li_{0.1}O$	12/14/90	-	2.3	Ni nit, Li nit
14. Cr-doped NiO	1/5/91	-	$3x10^6$	Ni nit, Cr nit
Ni-based perovskites				
15. $LaNiO_3$	07/12/90	-	-	La nit, Ni nit, Na_2CO_3
16. La_2NiO_4	08/06/90	-	-	La nit, Ni nit, Na_2CO_3
17. $LaSr_{.75}Ba_{.25}NiO_4$	08/21/90	-	-	La, Sr, Ni nit, Na_2CO_3
18. $La_4Ni_3O_{10}$	09/09/90	-	-	La, Ni nit, Na_2CO_3
19. La_2NiO_4	09/28/90	-	-	La, Ni nit, CA, ED
20. $LaNiO_3$	10/01/90	-	-	La, Ni nit, CA, ED

a. The resistivity measurements were made with the powders under a static load; the densities were 18~35% theoretical.
b. Abbreviations: nit = nitrate; carb = carbonate; ac = acetate; CA = citric acid; ED = ethylene diamine.

Appendix 3

Chapter 8 in "Electrochemistry in Transition," O. J. Murphy, S. Srinivasan and B. E. Conway, Editors, Plenum Press, in press (1991).

Transition Metal Oxide Electrocatalysts for O_2 Electrodes: The Pyrochlores

by Jai Prakash, Donald Tryk, Wesley Aldred and Ernest Yeager

TABLE OF CONTENTS

Transition Metal Oxide Electrocatalysts for O_2 Electrodes: The Pyrochlores

by Jai Prakash, Donald Tryk, Wesley Aldred and Ernest Yeager

Case Center for Electrochemical Sciences
and the Chemistry Department
Case Western Reserve University
Cleveland, Ohio 44106-7078

1. INTRODUCTION

There has been wide interest in the search for bifunctional oxygen electrocatalysts which can reversibly or nearly reversibly catalyze both the reduction and generation of O_2. There are two possible approaches: 1) a single bifunctional electrocatalyst which promotes both reactions; and 2) separate electrocatalysts for the two reactions within one electrode. Both approaches have been tried by various groups. The use of separate catalysts for these two functions provides a much wider range of materials for consideration. In this chapter, however, the first approach will be emphasized, with the focus on the transition metal pyrochlore oxides, particularly the lead ruthenate pyrochlore and related materials. These pyrochlores have metallic conductivity, can be prepared in very high area forms and also show high electrocatalytic activity for both O_2 reduction and generation.[1-4] The nature of the electrocatalysis is also very much dependent on the surface electronic properties of the catalyst, which in turn are dependent to some extent on the bulk properties.

This chapter will review some of the results obtained by various research groups, including the authors', for the lead, bismuth, yttrium and rare earth ruthenates concerning their electronic, electrochemical and electrocatalytic properties, especially for O_2 reduction and generation. Areas to be described include the use of ionomer membranes to stabilize pyrochlore-based gas-fed electrodes, use of high area carbon as a support material in gas-fed electrodes and the optimization of the structure of self-supporting gas-fed electrodes.

Much of the effort in the authors' laboratory has been focused on the stoichiometric lead ruthenate $Pb_2Ru_2O_{7-y}$ as a model compound because of its relative simplicity. Additional advantages are that its electronic conductivity is higher than that for the lead-rich compounds,[5] and its stability in concentrated alkaline solution is also higher.[2,3] Horowitz et al.[2,3] have concluded that the catalytic properties for the lead ruthenates are not strongly dependent upon composition but simply depend upon the surface area. They have favored the lead-rich compounds because they can be prepared more readily in high area form,[2,3,6-8] although they have also been able to prepare the stoichiometric compound in high area form (150 $m^2\ g^{-1}$, Ref. 8). The authors' research group has also been able to prepare the stoichiometric compound in relatively high area forms.

2. STRUCTURAL, PHYSICAL AND CHEMICAL PROPERTIES

2.1. General

The pyrochlores can be represented by the formula $A_2B_2O_6O'$, where A is typically a rare earth or an element such as Tl, Pb or Bi, B is typically a transition or post-transition metal, and O and O' are crystallographically distinct types of oxygen. Vacancies can occur at the O' sites, and other anions such as fluoride can also be substituted at these sites. Thus there are three different types of sites, A, B and O', in which substitutions can be made as long as the ionic radii are appropriate and charge neutrality is maintained. Consequently a large number of different pyrochlores exist with a wide range of physical properties.[9] The $A_2B_2O_7$ type of pyrochlore has been referred to as the stoichiometric or normal type as opposed to the defect pyrochlores, for which vacancies can exist, both in A and O'. With A cations such as Tl^+, Pb^{2+} and Bi^{3+}, O' vacancies can occur, resulting in the formula $A_2B_2O_{7-y}$. It has been argued[10,11] that the existence of O' vacancies is favored by the formation of A-A metal-metal bonds across these vacancies, although this view has also been argued against, as will be discussed below. In any case, the O' vacancies are thought to be central to the electronic and electrocatalytic properties of these pyrochlores.

Another variant of the pyrochlore structure is one in which part of the B sites are substituted with A-type cations. This occurs for example with lead and bismuth-based pyrochlores. These Pb-rich and Bi-rich compounds, particularly ruthenates and iridates, have been investigated by Horowitz and coworkers for their electrocatalytic properties[1,3] as well as their precisely controllable resistivities.[5]

2.2. Preparation

Randall and Ward[12] were the first to report the synthesis of Pb-Ru and Pb-Ir oxides with the pyrochlore structure. These compounds actually had Pb/Ru and Pb/Ir molar ratios of 2:1 and were thus lead-rich. Subsequently the stoichiometric lead ruthenate $Pb_2Ru_2O_{7-y}$ and lead iridate $Pb_2Ir_2O_{7-y}$ were prepared by Sleight[13] and Longo et al.[10] These syntheses were traditional solid-state-type ceramic preparations. In order to promote the diffusion of ions during the synthesis and thereby approach a homogeneous composition, the materials were subjected to prolonged high temperature heat treatments. In this process, however, the surface areas were considerably decreased. Chemically bound water would also tend to be driven off. Materials prepared in this way tend to exhibit relatively low catalytic activities. The full catalytic activity of the pyrochlores was not realized until Horowitz et al.[6,7] reported the synthesis of lead and bismuth ruthenates with quite high surface areas, ranging from 50 to 200 $m^2\ g^{-1}$. They used an alkaline aqueous solution as both a means of reacting the appropriate metal cations by precipitation and subsequently as a medium for the crystallization of the precipitate. The presence of oxygen in the solution was used to control the oxidation state of the cations. The important factors controlling the alkaline solution synthesis,

particularly the composition (i.e., A cation substitution at B cation sites) and surface area, are: 1) the solubilites of the A and B cations, which are often in complex anionic forms; 2) pH; 3) temperature; and 4) effective redox potential of the solution environment. The high solubility of lead species relative to ruthenium species, especially with increasing pH and temperature, must be taken into account.[3,6,7] Thus, an excess of lead salt must be used in many cases. To favor the formation of the stoichiometric lead ruthenate $Pb_2Ru_2O_{7-y}$, the concentration of lead in solution should be kept low by replacing the alkaline solution medium periodically with fresh solution.[8] If, however, there is insufficient lead to form the stoichiometric pyrochlore, an impurity phase of RuO_2 can form. The formation of RuO_2 was also found to be favored when the pH, temperature and O_2 partial pressure were all lower than optimum for the pyrochlore.[14]

The relatively low synthesis temperature (70-90°C) used in the alkaline solution technique yields pyrochlores with quite high surface areas.[6-8] The authors have been able to prepare crystalline $Pb_2Ru_2O_{7-y}$ with a surface area of 35 $m^2\ g^{-1}$ even without further heat treatment. More recent preparative efforts using the same technquiques in this laboratory have achieved crystalline material with a surface area of 105 $m^2\ g^{-1}$.[15]

2.3. Crystal Structure

There are several different ways of describing the pyrochlore structure. As pointed out by several authors,[9,16,17] this is partly due to the fact that the coordination polyhedra of O^{2-} anions surrounding the A and B cations change shape as a function of the variable positional parameter x_O for the oxygens in the BO_6 polyhedra (Fig. 1). At one extreme, x_O can in principle take the value 0.3125 (origin at the B cation) or 0.75 - 0.3125 = 0.4375 (origin at the A cation), in which case the BO_6 polyhedra are regular octahedra. At the other extreme, x_O can take the value 0.375 (either A or B origin), in which case the BO_6 polyhedra are highly distorted octahedra, but the AO_8 polyhedra are regular cubes. In the latter case, the structure is similar to the body-centered cubic fluorite structure.[10] The practical range for x_O is actually 0.305 to 0.355.[18] The x_O parameter for $Pb_2Ru_2O_{6.5}$ has been established to be 0.3232 (B-origin) or 0.4268 (A-origin) by Beyerlein et al.[19] This value is 83% of the way towards the regular octahedron extreme. Thus the description based on BO_6 octahedra is appropriate for this material.

The BO_6 octahedra are corner-shared and are in a diamond-like network.[16] Figure 2 shows two tetrahedral clusters of such a network. From this figure it can be seen that the B-O-B angle is not 180° as it would be in an ideal perovskite structure. Instead it is 135° (141° for regular octahedra), which affects the overlap of the B and O atomic orbitals that form the metal-like d band [10,11,20] and also affects the orientations of the d-like orbitals on the surface.

Not shown in the figure is the interpenetrating diamond-like A_2O' network, in which the O' atoms are at the vertices of the zig-zag -O'-A-O'-A- chains[18] as in cuprite.[16] The O' anions are located at the Fig.

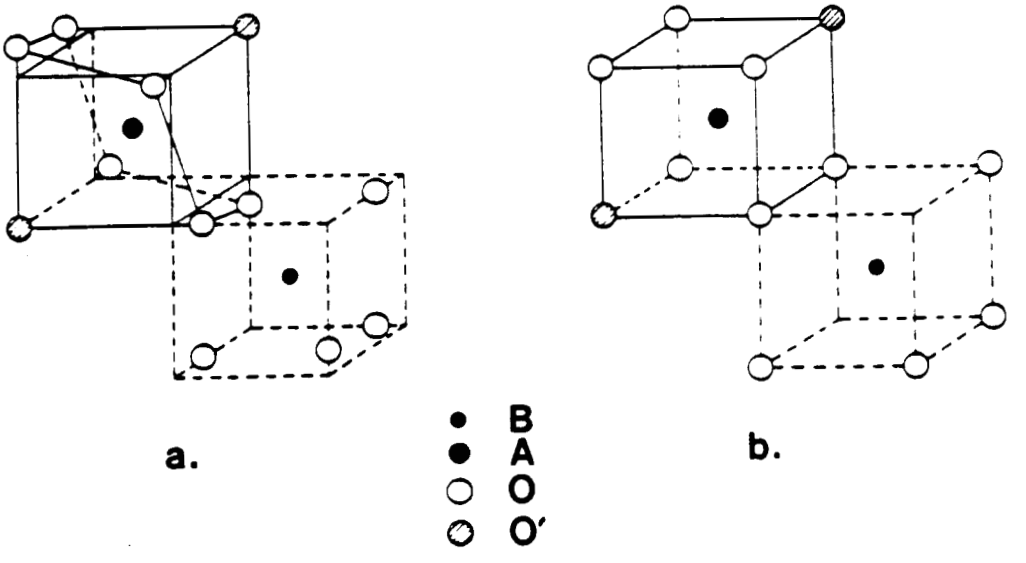

Fig. 1. Changes in the shapes of the coordination polyhedra of the A cations (e.g., Pb^{2+}) and B cations (e.g., $Ru^{4.5+}$) with the oxygen positional parameter x_0 (48f oxygens in the space group Fd3m) in the $A_2B_2O_6O'$ structure: a) $x_0 = 0.3125$ (origin at the B cation); b) $x_0 = 0.375$. Taken from Subramanian et al. (Ref. 9).

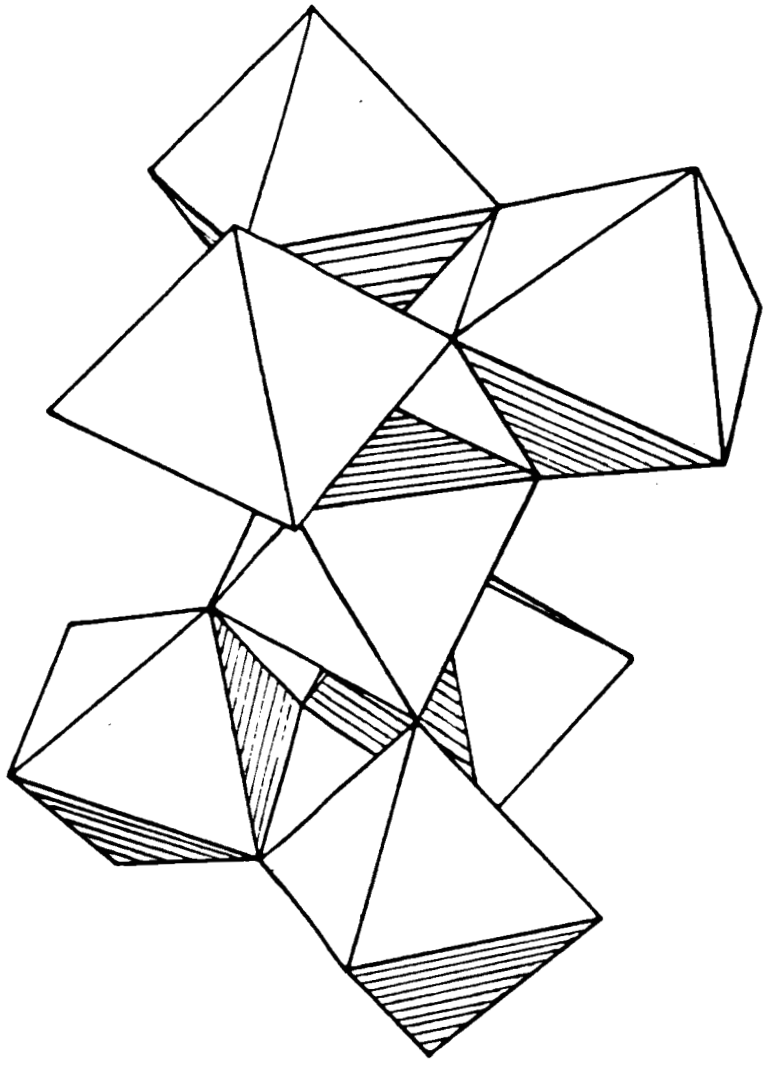

Fig. 2. Schematic of the pyrochlore structure, showing only the corner-shared BO_6 polyhedra (somewhat distorted octahedra), forming two interlocking tetrahedral clusters of a diamond-like network. Not shown is the inter-penetrating A_2O' diamond-like network.

centers of the large voids in the B_2O_6 network. In the anion-deficient pyrochlore structure exemplified by $Pb_2Ru_2O_{6.5}$ (or $Pb_2Ru_2O_6O'_{0.5}\square_{0.5}$), half of the O' atoms are missing. Beyerlein et al.[19] found using neutron diffraction that these vacancies are ordered, alternating along each chain: -A-O'-A-□-. The Pb atoms are shifted towards the vacancies symmetrically and also symmetrically away from the O' anions. This leads to a slightly more complex form of symmetry, because in the ideal pyrochlore structure, which belongs to the Fd3m space group, the A cation and O' anion positions are fixed, and the O' vacancies are assumed to be randomized. With the ordering of the vacancies and the associated movement of the A cations, the structure then belongs to the $F\bar{4}3m$ space group.[19]

Goodenough and coworkers have proposed that there is a bonding interaction between Pb cations across the the O' vacancies and that this interaction affects the electronic properties such as the electronic conductivity and the density of states (DOS) at the Fermi level E_F.[10,11] Specifically the Pb 6s electrons were thought to be involved in an O' vacancy-mediated or "trap-mediated" bond. Such bonds were also thought to stabilize the pyrochlore structure as compared with the perovskite structure. An alternate explanation has been proposed for the stabilization of the anion-deficient pyrochlore structure by Sleight,[21] who stated that the pyrochlore structure allows the oxygen anions to have strong covalent bonds to four nearest neighbors in a nearly tetrahedral arrangement. This can only occur for A and B cations that are not strongly electropositive. This argument is able to explain the existence of the pyrochlore $Ag_2Sb_2O_6$, in which oxygen vacancy-mediated bonds could not occur due to the lack of lone-pair electrons.[22]

There are also more recent indications of problems with the oxygen vacancy-mediated bond model, specifically in the neutron diffraction data of Beyerlein et al.[19] and in the band structure calculations and UPS measurements of Hsu et al.[23] (discussed below).

2.4. Physical Properties

As noted by several authors, the electronic and magnetic properties of the pyrochlores vary over a wide range (see Ref. 9). Even among the ruthenate pyrochlores, Goodenough and coworkers[11] point out that the electronic conductivities range from semiconducting to metallically conducting and the magnetic behavior from moderately temperature-dependent paramagnetism, due to localized electrons, to very low-level, essentially temperature-independent (Pauli-type) paramagnetism due to delocalized conduction electrons in metallic conductors (see Table 1). For example, lead ruthenate has very low resistivity together with a positive thermal coefficient of resistance (TCR) and Pauli-type paramagnetism. These metal-like properties have been rationalized by both Cox et al.[11] and by Hsu et al.[23] as being due to broadening of the partially-filled Ru 4d t_{2g} band. Cox et al.[11] proposed that the band broadening comes about due to interaction of the Ru 4d obitals with the Pb 6s orbitals through the framework oxygens, while Hsu et al.[23] considered that the band is broadened through interaction between Ru 4d and O 2p orbitals, with further broadening due to an interaction with

Table 1
Electrical and Magnetic Properties of Selected Ruthenate Pyrochlores

compound	sample type	ρ_{298},[a] Ω cm	TCR,[b] ppm	magnetic behavior	references
$Pb_2Ru_2O_{6.5}$	sinter	2.7×10^{-4}	-	Pauli paramagnetic	10
	sinter	5×10^{-4}	-	-	13
	sinter	2.0×10^{-3}	-	-	24
	sinter	3.0×10^{-4}	-	-	25
	powder	1.2×10^{-3}	+1700	-	5
	sinter	4.7×10^{-4}	+2770	-	26
$Y_2Ru_2O_7$	sinter	2.7×10^{-3}	-	-	25
	powder	-	-	paramagnetic	27, 28
$Nd_2Ru_2O_7$	single crystal	2.0	negative	-	20
	sinter	4.2×10^{-3}	-	-	25
	powder	-	-	paramagnetic	27
$Dy_2Ru_2O_7$	sinter	4.4×10^{-3}	-	-	25
	powder	-	-	paramagnetic	27

a. Resistivity at 298 K.

b. Thermal coefficient of resistivity, in 10^{-6} cm cm^{-1} K^{-1}

unoccupied Pb 6p orbitals. Yttrium ruthenate, on the other hand, is a somewhat poorer conductor and exhibits paramagnetic behavior due to localized unpaired electrons. This has been rationalized by Cox et al.[11] as being due to competition between Ru 4d and Y valence orbitals for oxygen p electrons, thus narrowing the conduction band. Hsu et al.[23] have also carried out band calculations for $Y_2Ru_2O_7$, which indicated that the Y 5s and 5p bands are too high in energy to play a significant role in band broadening and thus the t_{2g} band is narrow. Both groups are in agreement that the Y 5s and 5p levels are generally higher in energy than the Pb 6s and 6p levels, and the main point of disagreement is the energy of the Pb 6s and 6p levels in relation to the Ru 4d levels and thus the degree of mixing.

The rare earth ruthenates, for example, $Nd_2Ru_2O_7$ and $Dy_2Ru_2O_7$, have electrical and magnetic behavior similar to that of $Y_2Ru_2O_7$ (Table 1). There is a somewhat puzzling discrepancy, however, between the resistivities reported for $Nd_2Ru_2O_7$ single crystal[20] and presumably polycrystalline samples.[27] The difference is more than the expected scatter seen for example for the lead ruthenate resistivities (Table 1) and is much greater than the difference expected on the basis of single crystal vs. polycrystalline character. For example, such a difference is less than an order of magnitude for $Bi_2Ru_2O_{7-y}$.[20] In any case, on the basis of their magnetic behavior, the yttrium and rare earth pyrochlores are not expected to be metallic conductors.

Both Cox et al.[11] and Hsu et al.[23] showed that there is a relatively high DOS at E_F for $Pb_2Ru_2O_{6.5}$ as indicated by UPS. Cox et al. showed that $Y_2Ru_2O_7$ has an insignificant DOS at E_F. In their band calculations, Hsu et al. also found that $Y_2Ru_2O_7$ has a very small Y DOS at E_F.

As will be discussed later, $Y_2Ru_2O_7$ as well as $Nd_2Ru_2O_7$ and $Dy_2Ru_2O_7$ have very low catalytic activities for O_2 reduction and generation, while $Pb_2Ru_2O_{7-y}$ is very active for both reactions. With the data available at present, it is tempting to speculate that the differences in catalytic activity are related to the differences in DOS at E_F.

3. ELECTROCHEMICAL AND ELECTROCATALYTIC PROPERTIES

3.1. Electrochemical Properties

The intrinsic electrochemical behavior of the stoichiometric lead ruthenate pyrochlore $Pb_2Ru_2O_{7-y}$ in alkaline solution is somewhat complicated and is still not completely understood. Several groups have presented cyclic voltammetry,[29-31] including the authors',[4], with varying interpretations. An additional complicating factor is that the shapes of the CV curves are probably somewhat dependent upon the details of the oxide preparation, electrode fabrication as well as other factors such as potential cycling history.

The electrochemical behavior has some similarities with that of thermally prepared RuO_2, in that the charge under the voltammetric curve is probably due at least in part to a series of redox processes involving multiple electron transfers to the Ru cations.[32,33] The lead in the pyrochlore may also undergo redox processes. The CV charge for the pyrochlore is only slightly dependent upon the potential sweep rate

at least for low area samples. This is different from the behavior of the RuO_2 films, which can have substantial sweep rate dependence.[33,34]

The anodic sweep in the CV for a thin PTFE-bonded layer of $Pb_2Ru_2O_{7-y}$ exhibits a series of small peaks apparently superimposed on a gradually increasing background (Fig. 3). The total anodic charge over the potential range -0.68 to +0.52 V vs. Hg/HgO was approximately 2.1 x 10^4 C mol^{-1} of Ru (0.22 Faradays per mole of Ru). The cathodic charge was very similar, 2.2 x 10^4 C mol^{-1} Ru (0.24 Faradays per mole Ru), indicating negligible amounts of excess anodic charge, which can arise due to O_2 generation and electro-dissolution. An average surface coverage of both Ru and Pb cations on the oxide particles might be considered to be ~7 x 10^{-10} mol cm^{-2} [7.3 x 10^{-10} mol cm^{-2}, averaged for (111) and (222) surfaces, and 6.3 x 10^{-10} for the (100) surface] or 6.8 x 10^{-5} C cm^{-2} for each Ru or Pb cation, assuming one electron transfer, while the experimental charge was 3.5 x 10^{-3} C cm^{-2}, a factor of ~50 higher. The possible redox proceses in this potential range include (Refs. 36-40: Ru; Refs. 41-43: Pb):

$$Pb^{2+} \xrightarrow{-2e^-} Pb^{4+}$$

$$Ru^{3+} \xrightarrow{-4e^-} Ru^{7+}$$

for a total of up to 6 electrons. Thus the charge developed might involve >9 layers of cations, which are spaced ~2.56 Å apart in the [100] direction.

The small superimposed peaks are thought to involve discrete redox processes occurring at the surface of the oxide particles. For example, the charge under the unresolved peaks c and d totaled ~1.4 x 10^{-4} C cm^{-2} (true area), which corresponds to ~2 electrons or ~1 electron for each peak. The areas under the other peaks cannot be measured precisely but are also in the one-electron range. These peaks unfortunately cannot be unequivocally assigned to particular redox processes due to the uncertainty in the hydration of the surface. The voltammetry in acid solution and at intermediate pH may aid in the interpretation of these peaks. Preliminary work in the authors' laboratory has shown that there are peak potential shifts with pH over the range ~12 to 14, but these shifts may partially be complicated by local pH shifts within the porous layer due to lack of buffer capacity.

Goodenough et al.[31] have recently presented the voltammetry of $Pb_2Ru_2O_{7-y}$ in acid solution, which shows the presence of three redox couples. These were assigned as follows: E_0 ~ +0.33 V (SHE) to Ru^{2+}/Ru^{3+}; E_0 ~ +1.14 V (SHE) to Ru^{3+}/Ru^{4+}; and E_0 ~ +1.38 V (SHE) to Ru^{4+}/Ru^{5+}. At pH 14 (assuming 0.06 V per pH unit), the +1.14 V peak would be expected to shift to ~+0.31 V and the +1.38 V peak to ~+0.55 V. These potentials are in reasonably good agreement with E_0 values obtained in our voltammetry of +0.32 V (SHE) and +0.48 V (SHE) (Fig. 3). Different samples of $Pb_2Ru_2O_{7-y}$ have also shown deviations from these values, so that the ranges are +0.28 ~ +0.32 V and +0.46 ~ +0.48 V.

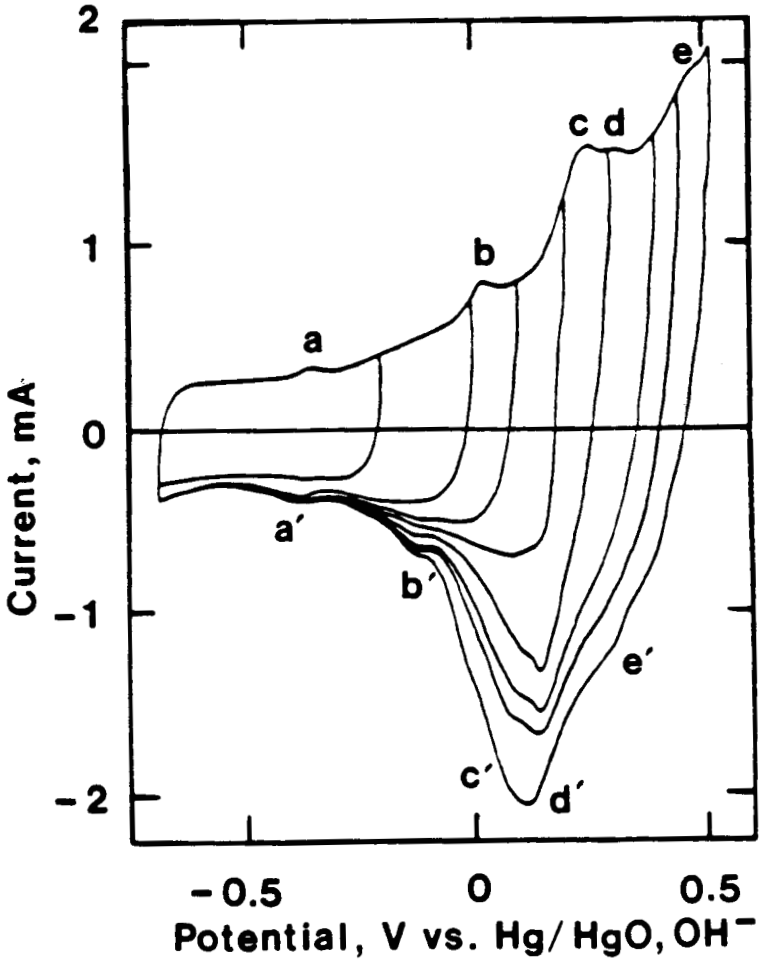

Fig. 3. Cyclic voltammetry for $Pb_2Ru_2O_{7-y}$ pyrochlore in the form of a thin PTFE-bonded porous coating on the basal plane of pyrolytic graphite disk in N_2-saturated 1.0 M KOH at 22°C. The coating contained 4.0 mg cm^{-2} pyrochlore and 0.2 mg cm^{-2} Teflon T30B; electrode area was 0.196 cm^{-2}; sweep rate was 20 mV s^{-1}.

The +0.04 V (SHE) peak (Fig. 3) occurs in the same region as the onset of O_2 reduction, but this peak does not occur in all $Pb_2Ru_2O_{7-y}$ samples. Thus the possible involvement of discrete redox couples in the O_2 reduction is still in question.

In the future the use of in situ spectroscopic techniques may shed further light on the assignment of specific voltammetric peaks as well as the overall process, which may involve some of the bulk structure of the oxide. Mössbauer spectroscopy could be a particularly powerful technique in identifying the ruthenium valency and spin states. Another technique that could be quite powerful in this regard is XANES.

3.2. Electrocatalysis - General Aspects

Although the principal emphasis in this review is on the O_2 reduction and generation reactions, it is worth noting that the lead and bismuth ruthenate pyrochlores have electrocatalytic activity for other reactions. The first documented use of pyrochlores of this type as electrocatalysts was by Welch in 1974[43] for chlorine generation. He also recognized their possible application for a wide range of other electrolytic processes in which dimensionally stable anodes are needed. Most of the other examples of electrocatalysis involve organic oxidation reactions, including alkenes,[3,7,30] monosaccharides and lignins,[44] alcohols[3,7,45] and ketones.[7] The remainder of this review will be devoted to the oxygen reduction and generation reactions. These are of special interest due to their involvement in fuel cells, energy storage systems and industrial electrolysis.

3.3. O_2 Reduction

The kinetic analysis for O_2 reduction was carried out using a graphite disk - gold ring rotating electrode with a thin Teflon PTFE-bonded coating of $Pb_2Ru_2O_{7-y}$ on the disk.[4] O_2 transport with such electrodes involves transport through the bulk solution to the porous electrode and transport within the electrode in gas-filled pores. The effectiveness of the O_2 transport within the electrode is very great. The active catalyst layer is only of the order of a few microns in thickness. The standard treatments of the rotating disk and ring-disk electrode techniques must be used with caution, however.

The disk and ring currents at several rotation rates are shown in Fig. 4. The plots of $(\text{current})^{-1}$ vs. $(\text{rotation rate})^{-1/2}$ based on the data in Fig. 4 were linear (Fig. 5). The slopes (inversely related to the Levich B coefficient) can be used to determine the overall number of electrons transferred, n. The apparent n value, ~3.8, was relatively independent of rotation rate and potential over the potential range -0.04 to -0.1 V vs. Hg/HgO, OH^-. The ring currents for peroxide oxidation were essentially zero for the first ~100 mV after the onset of O_2 reduction. Thereafter they rose to a maximum of ~5% of the disk current (after correction for the collection efficiency). Unfortunately, however, the porous character of the coating precludes a confident quantitative analysis of the ring data. This is because peroxide can be produced in the catalyst pores and then be decomposed at the pore walls before having an opportunity to diffuse into the bulk solution. The transport of peroxide out of the porous

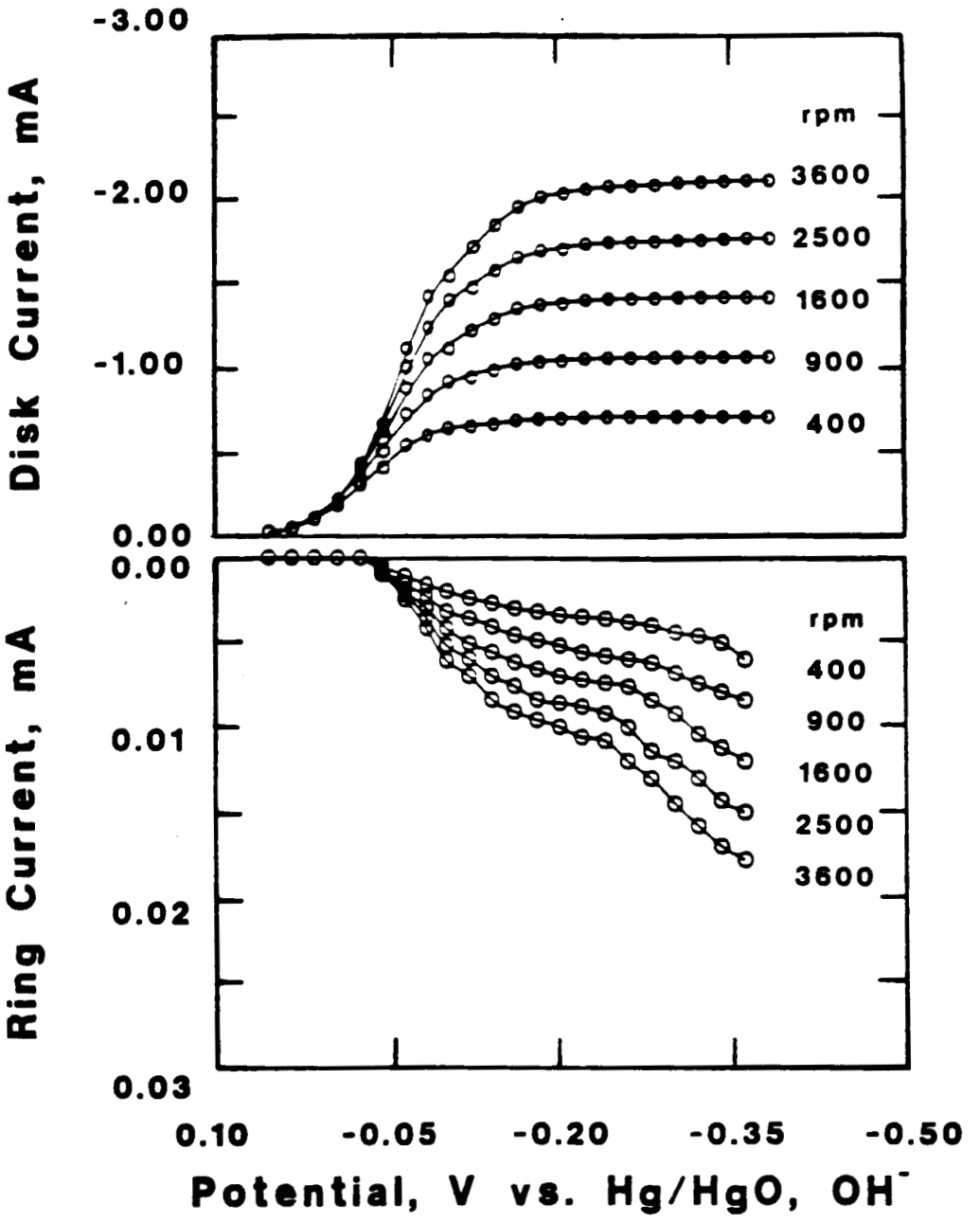

Fig. 4. Rotating ring-disk polarization curves (steady state) for O_2 reduction on a thin PTFE-bonded porous coating of $Pb_2Ru_2O_{7-y}$ in O_2-saturated 1.0 M KOH at 22°C. The composition of the coating was as shown in Fig. 3. Electrode area was 0.45 cm^2; collection efficiency was 0.177; rotation rates were as shown.

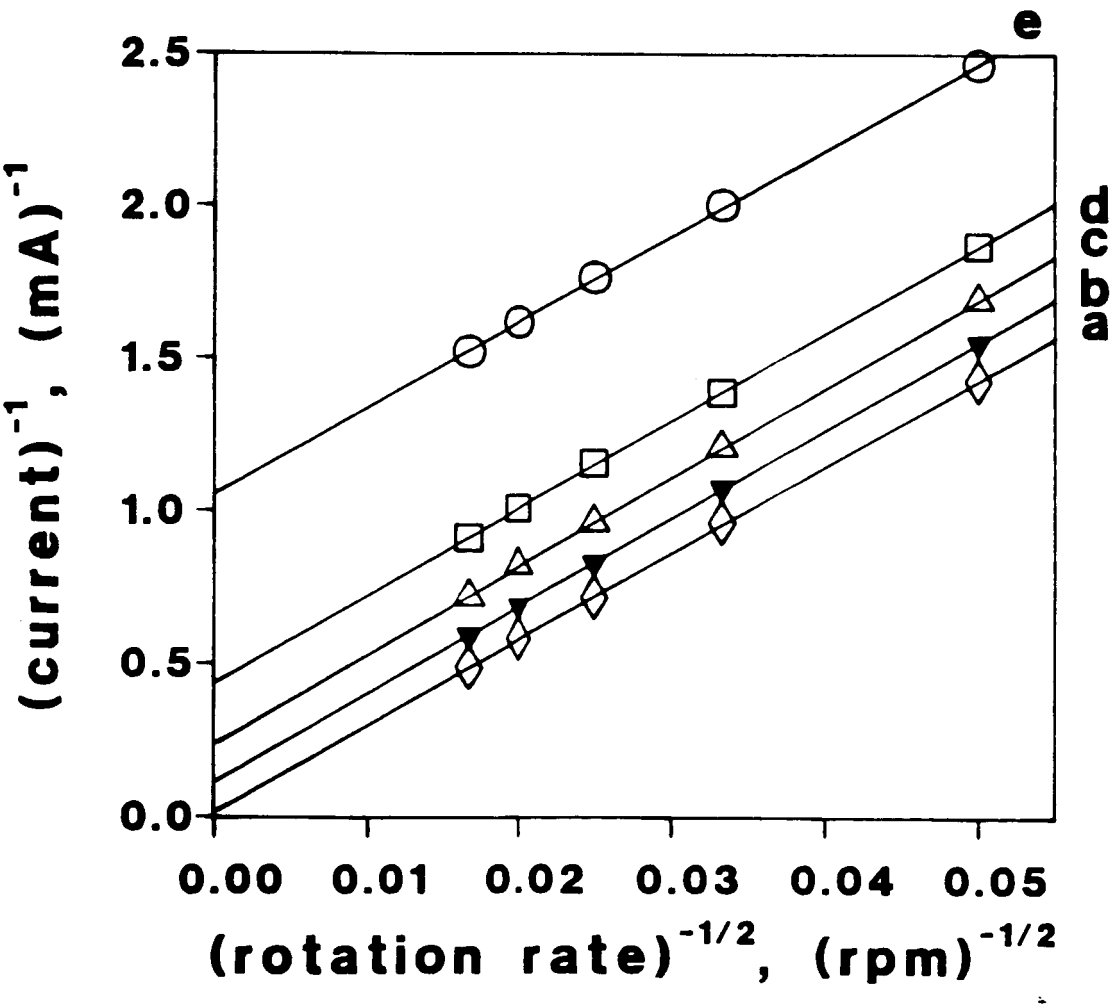

Fig. 5. (Current)$^{-1}$ vs. (rotation rate)$^{-1/2}$ plots for O_2 reduction on a rotating disk electrode with a thin Teflon-bonded coating of $Pb_2Ru_2O_{7-y}$ based on the data of Fig. 4: a) -0.4 V; b) -0.1 V; c) -0.08 V; d) -0.06 V and e) -0.04 V vs. Hg/HgO, OH^-.

electrode is likely to be very restricted because of slow diffusion within the active catalyst layer for a solution phase component. Thus it remains open to question as to whether the pyrochlore is catalyzing the direct 4-electron reduction of O_2 or is just a very efficient peroxide decomposer. Experiments carried out in the authors' laboratory indicate that at least the latter is true. Further research must be done with non-porous forms of the catalyst in order to settle this question.

A mass transport-corrected Tafel plot (not shown) based on the data of Fig. 4 exhibited a linear portion over the potential range +0.04 to -0.10 V vs. Hg/HgO with a slope of -0.063 V (decade)$^{-1}$. This slope could indicate a) a rate-determining first electron transfer step involving an adsorbed product such as OH^- with Temkin adsorption behavior or b) a rate-determining chemical step following a fast first electron transfer step. A redox mediator mechanism would be an example of the latter.

The effect of pH variation (11.9 to 13.9) on the O_2 reduction was examined and the reaction order in OH^- concentration was found to be -0.50 ± 0.02. The slopes of the mass transport-corrected Tafel plots on which this reaction order was based were nearly identical, providing evidence that the reaction mechanism remained the same over this pH range.

The reaction order of -0.5 together with the -0.06 V (decade)$^{-1}$ Tafel slope are consistent with the data of Egdell et al.,[29] which was explained as follows. First there is proposed to be a fast outer-sphere reduction of O_2 to O_2^- followed by protonation to yield physisorbed HO_2. This then displaces a surface OH^- in the rds. An electrostatic argument was invoked to explain the -0.5 reaction order for OH^-.

In more recent work of Goodenough et al. at pH extending from acid to base,[31] the mechanism for O_2 reduction on $Pb_2Ru_2O_{7-y}$ at pH > 2 was proposed to involve the following:

$$O_2 + e^- \longrightarrow (O_2^-)_{ads} \qquad (1)$$

$$Pb^{2+}OH^- + (O_2^-)_{ads} \longrightarrow Pb^{2+}O_2^- + OH^- \quad (rds) \qquad (2)$$

$$Pb^{2+}O_2^- + 2H_2O + 3e^- \longrightarrow Pb^{2+}OH^- + 3OH^- \qquad (3)$$

Surface charge density vs. pH measurements indicated that the oxygens in the Ru_2O_6 framework are not protonated at higher pH and thus are not labile enough to undergo exchange with O_2^-.[31] At pH below 2, the Ru-bound oxygens become protonated and the Ru^{3+} cations can then take part in a step analogous to reaction 2.[31] Steps such as this (e.g., reaction 2), not involving charge transfer, are consistent with the observed Tafel slope (~-0.06 V/decade). Reaction 3 is consistent with a lack of peroxide generation. The -0.5 reaction order for OH^- remains to be explained, however.

In order to fully elucidate the mechanisms for both O_2 reduction and generation on $Pb_2Ru_2O_{7-y}$, other factors may have to be taken into account, such as the specific steric-electronic environment on the

surface of the oxide. In this regard it should be helpful to examine the structure of the various surfaces both theoretically and experimentally in future work.

As a first step in this direction, one could look at the surface just as a simple termination of the bulk structure, realizing that this may be a gross oversimplification. A characteristic feature of both the (111) and (100) faces of $Pb_2Ru_2O_{7-y}$ is the zig-zag chains of RuO_6 polyhedra, with the Ru-O-Ru angle being 135° (Fig. 6). The octahedrally bound oxygens which point up and out of the surface are either inclined toward or away from each other. In the former case, these oxygens would ideally be about 2.8 Å from each other, assuming no relaxation of the structure at the surface. This can also be seen in more detail in Ref. 46. The zig-zag nature of the ideal pyrochlore surface is unique and distinguishes it from both the perovskite (e.g. $SrRuO_3$) and the rutile (e.g. RuO_2) structures. The proximity of these oxygens allows one to envision mechanisms in which breakage of the O-O bond in O_2 could be assisted by either these closely situated oxygens or by the Ru cations themselves. The details of such interactions remain to be worked out but would have to take into account the lack of protonation of the surface at high pH, as pointed out by Goodenough et al.[31]

3.4. O_2 Generation

The mechanism of the O_2 generation reaction on $Pb_2Ru_2O_{7-y}$ in alkaline solution also remains to be worked out in detail in the light of the surface structures. The mechanism that has been proposed by the authors' research group[4] involves adjacent Me-OH sites (probably Ru-OH) and, with the surface structure in mind, it is possible to imagine how this might work on the (111) surface (Fig. 7). The fact that the Ru cations are probably already 6-coordinate, as shown in I, means that the first step involves the formation of a 7-coordinate Ru species, which are known to exist as intermediates in some ligand substitution reactions.[47] Goodenough et al.[31] on the other hand have proposed a 6-coordinate $Me^{4+}O^{2-}$ intermediate (Me = Ir or Ru), which could be written alternatively as $Me^{4+}(O\text{-}O)^{2-}$.

In order to gain further understanding of the surface structure and how O_2, H_2O and OH- interact with it, it will be necessary to use some of the surface analytical techniques such as LEED, XPS, AES, SIMS and STM. The preparation of single crystal surfaces of pyrochlore oxides is not expected to be straightforward but should be well within the realm of possibility. One example of the expected problems is the fact that the (111) faces have 75% of the surface cations being Ru and 25% Pb, while the situation is reversed on the (222) faces. With the use of special etching techniques, it may be possible to handle such problems.

3.5. Gas-Fed Electrode Measurements

The performance of porous gas-fed O_2 electrodes based on Pb-Ru pyrochlores has been shown to be quite good in alkaline solution by several groups.[2,3,4,31] The O_2 generation performance has also been shown to be good.[2-4] One drawback to the use of these pyrochlores as electrocatalysts is their non-negligible equilibrium solubility in

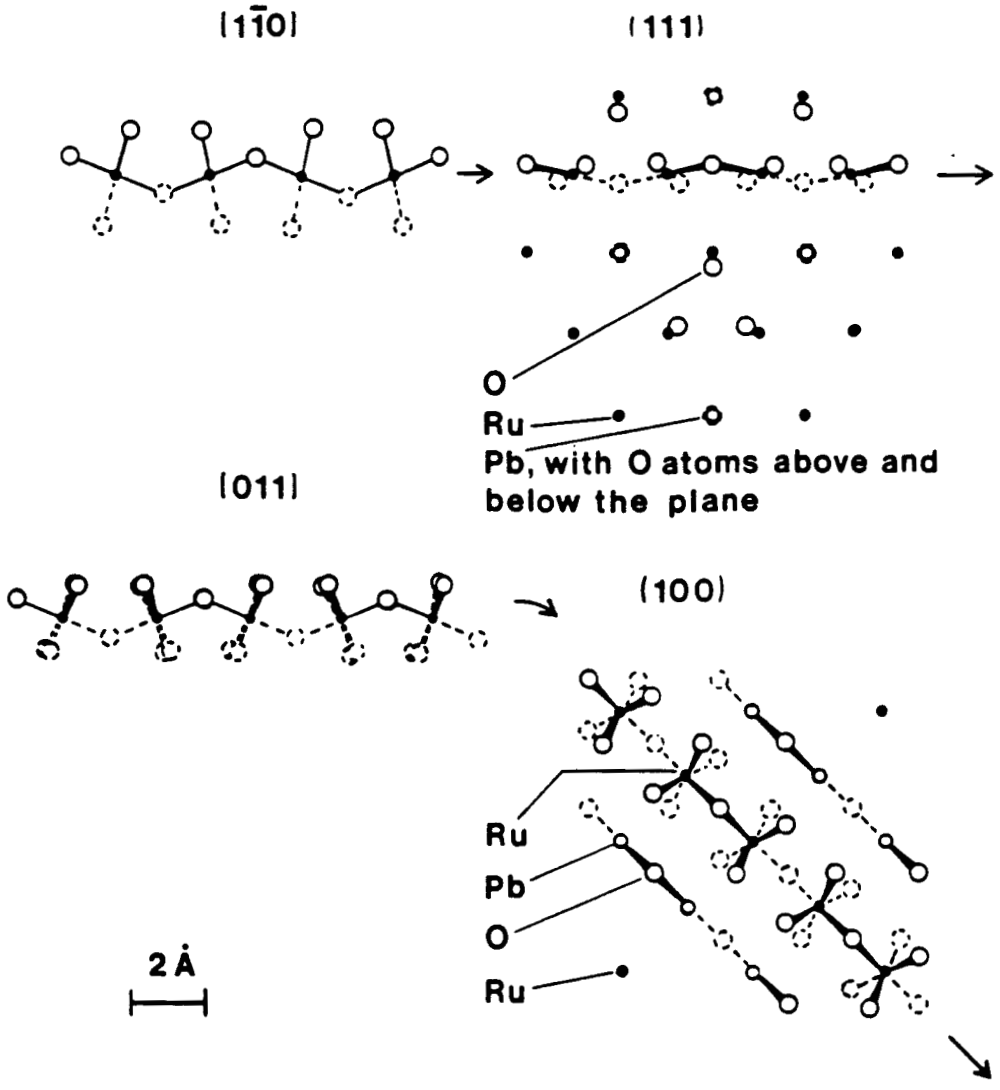

Fig. 6. Projections of the (111) and (100) surfaces of the $Pb_2Ru_2O_{7-y}$ pyrochlore (right side) and the zig-zag chains of corner-shared RuO_6 polyhedra in the indicated directions across these surfaces (left side). Dashed lines show atoms and bonds lying below the surface.

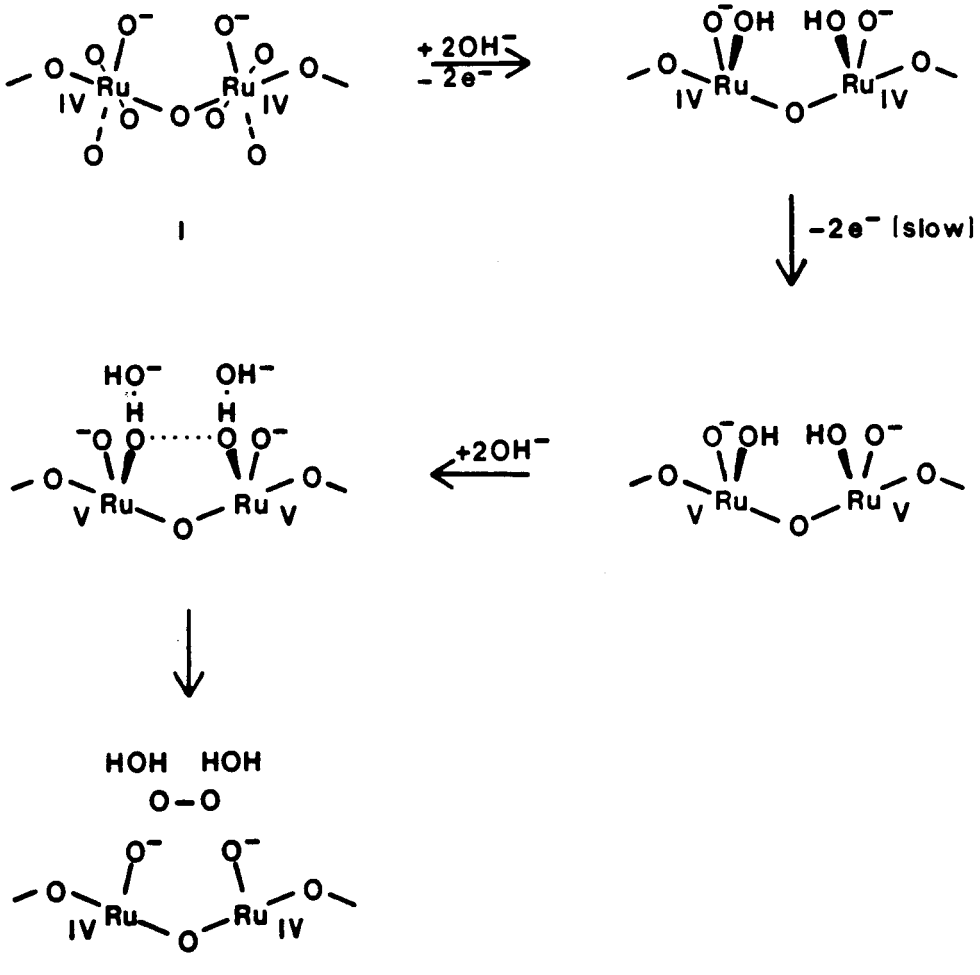

Fig. 7. Proposed mechanism for O_2 generation on the (111) face of $Pb_2Ru_2O_{7-y}$ in alkaline solution, showing a side-on view of two corner-shared RuO_6 polyhedra in the zig-zag chain shown in Fig. 6. In I, the three oxygens lying behind, below and in front of a Ru(IV) cation are shown but are omitted thereafter for clarity.

concentrated alkaline solution, which increases with more positive potentials.[2,3]

Both the electrocatalytic activity and the stability can be modified through the partial or complete substitution of the Pb and/or Ru cations. For example, as noted earlier, Pb can be replaced by Y or rare earth elements such as Nd or Dy. The resulting materials are paramagnetic semiconductors. The performance in both O_2 reduction and generation was found to be quite poor, which can be related either to their poor conductivity or to a low DOS at E_F. To some extent the poor performance was also a result of their low surface areas.

Part of the Ru can be substituted with Pb to form the "lead-rich" pyrochlores discussed earlier. The performance of gas-fed electrodes based on these compounds has been found to be superior to that of the stoichiometric pyrochlore $Pb_2Ru_2O_{7-y}$ but is related to the fact that the lead-rich compounds can be prepared in higher area form.[2,3] In our experience, however, the O_2 reduction performance of gas-fed electrodes made from the lead-rich compounds degrades much faster than that of the stoichiometric compound, especially when anodic polarization measurements are also made.

Part of the Ru can be substituted with Ir, and this is expected to modify the long-term stability. The performance on both O_2 reduction and generation of gas-fed electrodes based on such materials showed small improvements,[4] but the long-term stability has not been tested. There is some indication that partial substitution of the Ru with Sb can markedly improve the stability of Pb-Ru pyrochlores, especially in the more positive potential range.[48]

Other factors are also operative in determining stability. Such factors include the crystallinity and the presence of impurity phases such as RuO_2 and PbO. One can determine the importance of the crystallinity as long as one realizes that the crystallinity of a given sample cannot be improved without decreasing the BET surface area.

An alternate approach to stabilizing the pyrochlore involves the use of anion exchange polymers, both as a replacement for the liquid electrolyte phase within the porous electrode and as a discrete overlayer on the electrolyte side of the electrode.[49] Very encouraging results have been obtained using both techniques.[4] The diffusion of the ruthenate ion RuO_4^{2-} out of the porous electrode has been monitored spectrophotometrically during anodic polarization measurements, and a partially fluorinated anion exchange membrane (RAI 4035, RAI Corp., Hauppage, NY) was found to retard this process significantly.[50] The ion diffuses through the membrane relatively slowly probably due to size and electrostatic effects, although this needs further investigation.

A high area carbon support matrix has been used for some of the gas-fed electrodes fabricated in our laboratory. This has usually been an acetylene black (Shawinigan Black, Chevron Chemical Co., Olefins and Derivatives Div., Houston, TX; BET surface area ~ 80 $m^2\ g^{-1}$). This has been used mainly because it facilitates the fabrication of the Teflon-bonded porous electrodes. Although this carbon is comparatively oxidation-resistant in the O_2 generation mode,[51] other carbons have been developed that are even more corrosion- resistant,[52] such as that developed by Ross.[53] This carbon can also be used in gas-fed

electrodes in conjunction with pyrochlores, with little change in performance compared to that obtained with SB carbon.

Under conditions of high temperature and O_2 pressure, such as would be used in high performance alkaline fuel cells, it may be necessary to completely avoid the use of carbon matrices, however. Techniques have been developed in our laboratory to fabricate "self-supported" gas-fed electrodes based on $Pb_2Ru_2O_{7-y}$ and Teflon T30B.[15] The short-term performance for O_2 reduction and generation of such electrodes was very good (Fig. 8). Within the statistical accuracy of the measurement, the O_2 reduction current was first order with respect to the O_2 partial pressure over the range 1 to 10 mA cm^{-2}. Deviations in linearity of the polarization curve in the low current density range are probably associated with 1) surface redox couples on the pyrochlore and/or 2) rate-determining peroxide decomposition within the porous electrode. Deviations in the high current density range are most likely due to ohmic and/or mass transport limitations. Further improvements in electrode structures and fabrication techniques are needed.

The polarization curve for O_2 generation (Fig. 8b) was linear, with a Tafel slope very close to +0.04 V/decade. This is consistent with a rate-determining 2nd electron transfer step, as shown in the proposed mechanism in Fig. 7.

4. CONCLUSIONS AND RECOMMENDATIONS

The lead-ruthenium pyrochlores are promising electrocatalysts for O_2 reduction and generation in alkaline media. Their high catalytic activity may be associated with the relatively high density of electronic states at the Fermi level. Mechanisms by which these materials catalyze the O_2 reduction and generation reactions have been proposed but are far from certain. Specific ways in which the surface structures may be involved have also been proposed. Further fundamental research is needed to relate the electrocatalytic activity of the pyrochlores to their surface electronic and structural properties.

The lead-ruthenium pyrochlores have significant solubility in alkaline solution in the O_2 generation potential range, but the use of anion-conducting polymers, both as membrane overlayers and as an integral component of the gas-diffusion electrode, promises to alleviate this problem. Further improvements are also needed in gas-diffusion electrode fabrication techniques in order to achieve higher performance and stability.

Acknowledgements

This research was supported by grants from the U. S. Department of Energy through a subcontract with Lawrence Berkeley National Laboratory, from the NASA Lewis Research Center, and from the U. S. Air Force, Wright-Patterson AFB, through a subcontract with NASA-Lewis Research Center.

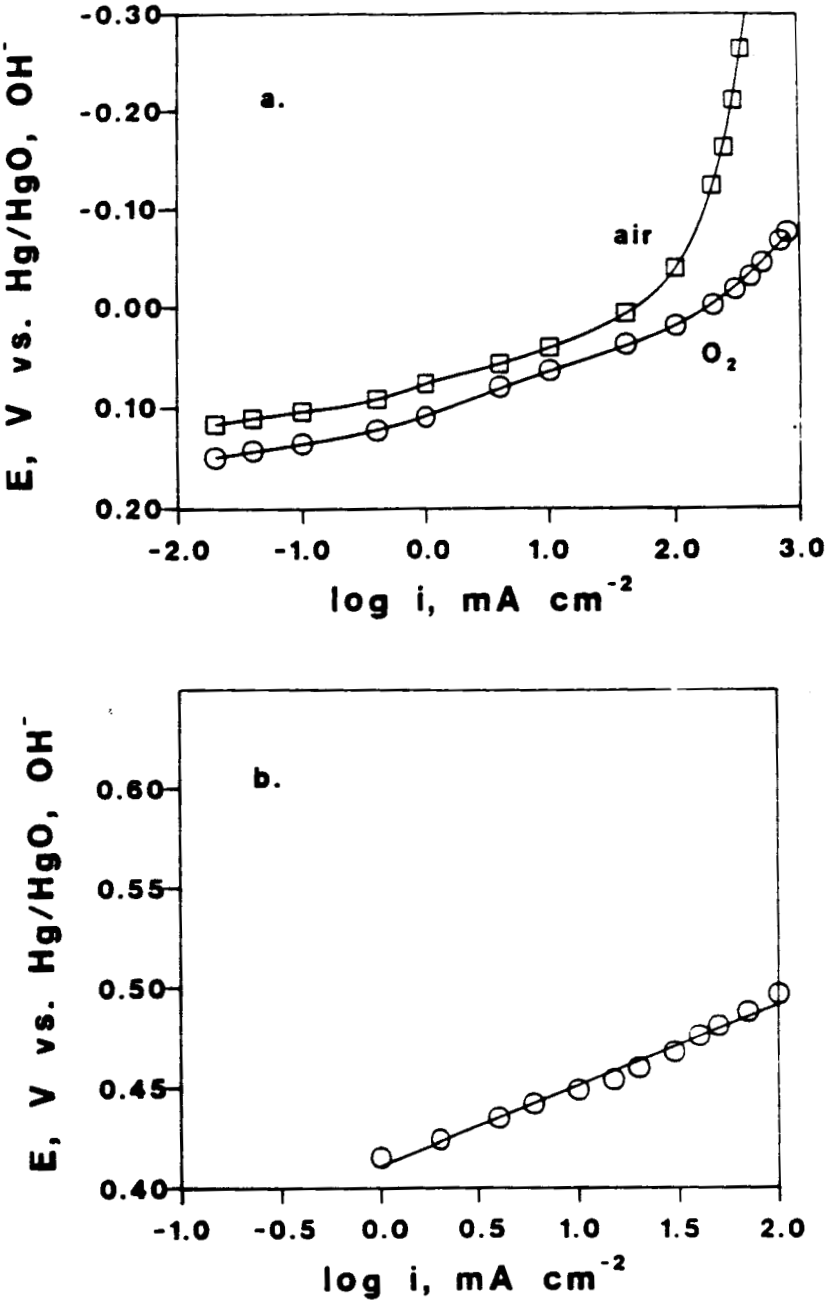

Fig. 8. Polarization curves for: a) O_2 reduction and b) O_2 generation with gas-fed (1 atm) electrodes based on $Pb_2Ru_2O_{7-y}$ pyrochlore in 5.5 M KOH at 25°C. The electrode in a) contained 83.3 mg cm^{-2} pyrochlore and 27.8 mg cm^{-2} Teflon T30B and was heat-treated at 330°C for 2 h in flowing helium. Ammonium bicarbonate (18.8 mg cm^{-2}) was added as a pore-former before the heat treatment. The b) electrode was made with a similar composition.

References

1. H. S. Horowitz, J. M. Longo and J. I. Haberman, $Pb_2[M_{2-x}Pb_x]O_{7-y}$ compounds wherein M is Ru, Ir or mixtures thereof, and method of preparation, U. S. Patent 4,124,539, November 7, 1978.
2. H. S. Horowitz, J. M. Longo and H. H. Horowitz, Oxygen electrocatalysis on some oxide pyrochlores, J. Electrochem. Soc., 130, 1851-1859 (1983).
3. H. S. Horowitz, J. M. Longo, H. H. Horowitz and J. T. Lewandowski, The synthesis and electrocatalytic properties of nonstoichiometric ruthenate pyrochlores, in: Solid State Chemistry in Catalysis (R. K. Grasselli and J. F. Brazdil, eds.), ACS Symposium Series 279, pp. 143-163, American Chemical Society, Washington, D. C. (1985).
4. J. Prakash, D. Tryk and E. Yeager, Electrocatalysis for oxygen electrodes in fuel cells and water electrolyzers for space applications, J. Power Sources, 29, 413-422 (1990).
5. R. A. Beyerlein, H. S. Horowitz and J. M. Longo, The electrical properties of $A_2[Ru_{2-x}A_x]O_{7-y}$ (A = Pb or Bi) pyrochlores as a function of composition and temperature, J. Solid State Chem., 72, 2-13 (1988).
6. H. S. Horowitz, J. M. Longo and J. T. Lewandowski, Method of making lead-rich and bismuth-rich pyrochlore compounds using an alkaline medium, U. S. Patent 4,129,525, December 12, 1978.
7. H. H. Horowitz, H. S. Horowitz and J. M. Longo, in: Electrocatalysis (W. E. O'Grady, P. N. Ross and F. G. Will, eds.), pp. 285-290, The Electrochemical Society, Pennington, NJ (1982).
8. H. S. Horowitz, J. M. Longo and J. T. Lewandowski, Method of making stoichiometric lead and bismuth pyrochlore compounds using an alkaline medium, U. S. Patent 4,176,094, November 27, 1979.
9. M. A. Subramanian, G. Aravamudan and G. V. Subba Rao, Oxide pyrochlores - a review, Prog. Solid State Chem., 15, 55-143 (1983).
10. J. M. Longo, P. M. Raccah and J. B. Goodenough, $Pb_2M_2O_{7-x}$ (M = Ru, Ir, Re) - preparation and properties of oxygen-deficient pyrochlores, Mat. Res. Bull., 4, 191-202 (1969).
11. P. A. Cox, R. G. Egdell, J. B. Goodenough, A. Hamnett and C. C. Naish, The metal-to-semiconductor transition in ternary ruthenium (IV) oxides: a study by photoelectron spectroscopy, J. Phys. C: Solid State Phys., 16, 6221-6239 (1983).
12. J. J. Randall and R. Ward, The preparation of some tenary oxides of the platinum metals, J. Am. Chem. Soc., 81, 2629-2631 (1959).
13. A. W. Sleight, High pressure synthesis of platinum metal pyrochlores of the type $Ab_2M_2O_{6-7}$, Mat. Res. Bull., 6, 775-780 (1971).
14. H. S. Horowitz, J. M. Longo and J. T. Lewandowski, Method of making lead and bismuth ruthenate and iridate pyrochlore compounds, U. S. Patent 4,203,871, May 20, 1980.
15. M. Shingler, W. Aldred, D. Tryk and E. Yeager, Final Report: Catalysts for Ultrahigh Current Density Oxygen Cathodes for Space Fuel Cell Applications, Contract No. NAG3-694 with NASA - Lewis Research

Center, prepared by Case Center for Electrochemical Sciences, Case Western Reserve University, May 1990.
16. A. F. Wells, Structural Inorganic Chemistry, 5th Edition, pp. 129, 258, Clarendon Press, Oxford (1984).
17. R. A. McCauley, Structural characteristics of pyrochlore formation, J. Appl. Phys., 51, 290-294 (1980).
18. A. W. Sleight, New ternary oxides of mercury with the pyrochlore structure, Inorg. Chem., 7, 1704-1708 (1968).
19. R. A. Beyerlein, H. S. Horowitz, J. M. Longo, M. E. Leonowicz, J. D. Jorgensen and F. J. Rotella, Neutron diffraction investigation of ordered oxygen vacancies in the defect pyrochlores, $Pb_2Ru_2O_{6.5}$ and $PbTlNb_2O_{6.5}$, J. Solid State Chem., 51, 253-265 (1984).
20. A. W. Sleight and R. J. Bouchard, Precious metal pyrochlores, in: Solid State Chemistry, NBS Special Publication 364 (R. S. Roth and S. J. Schneider, eds.), pp. 227-232, National Bureau of Standards, U. S. Dept. of Commerce, Washington, D. C. (1972).
21. A. W. Sleight, $AgSbO_3$: chemical characterization and structural considerations, Mat. Res. Bull., 4, 377-380 (1969).
22. R. J. Bouchard and J. L. Gillson, A new family of bismuth - precious metal pyrochlores, Mat. Res. Bull., 6, 669-680 (1971).
23. W. Y. Hsu, R. V. Kasowski, T. Miller and T. C. Chiang, Band structure of metallic pyrochlore ruthenates $Bi_2Ru_2O_7$ and $Pb_2Ru_2O_{6.5}$, Appl. Phys. Lett., 52, 792-794 (1988).
24. P. R. van Loan, Conductive ternary oxides of ruthenium and their use in thick film resistor glazes, Ceram. Bull., 51, 231-242 (1972).
25. V. B. Lazarev and I. S. Shlaplygin, Electrical properties of mixed oxides containing a platinum metal and a non-noble metal, Russ. J. Inorg. Chem., 23, 163-170 (1978).
26. G. Mayer-von Kürthy, W. Wischert, R. Kiemel, S. Kemmler-Sack, R. Gross and R. P. Huebener, System $Bi_{2-x}Pb_xPt_{2-x}Ru_xO_{7-z}$: a pyrochlore series with a metal-insulator transition, J. Solid State Chem., 79, 34-45 (1989).
27. R. Aleonard, E. F. Bertaut, M. C. Montmory and R. Pauthenet, Rare-earth ruthenates, J. Appl. Phys., 33 (supp.), 1205 (1962).
28. J. Rosset and D. K. Ray, Magnetic susceptibility of ruthenium-yttrium oxide ($Ru_2O_4 \cdot Y_2O_3$) powder, J. Chem. Phys., 37, 1017-1020 (1962).
29. R. G. Egdell, J. B. Goodenough, A. Hamnett and C. C. Naish, Electrochemistry of ruthenates. Part 1. Oxygen reduction on pyrochlore ruthenates, J. Chem. Soc., Faraday Trans. I, 79, 893-912 (1983).
30. J. A. R. van Veen, J. M. van der Eijk, R. de Ruiter and S. Huizinga, On the electrocatalytic properties of ruthenates, Electrochim. Acta, 33, 51- 57 (1988).
31. J. B. Goodenough, R. Manoharan and M. Paranthaman, Surface protonation and electrochemical activity of oxides in aqueous solution, J. Am. Chem. Soc., 112, 2076-2082 (1990).
32. L. D. Burke and O. J. Murphy, The electrochemical behavior of RuO_2-based mixed oxide anodes in base, J. Electroanal. Chem., 109, 199-212 (1980).

33. S. Ardizzone, G. Fregonara and S. Trasatti, "Inner" and "outer" active surface of RuO_2 electrodes, Electrochim. Acta, 35, 263-267 (1990).
34. L. D. Burke and O. J. Murphy, Cyclic voltammetry as a technique for determining the surface area of RuO_2 electrodes, J. Electroanal. Chem., 96, 19-27 (1979).
35. M. Pourbaix, Atlas of Electrochemical Equilibria in Aqueous Solutions, pp. 343-349, Pergamon, Oxford (1966).
36. J. F. Llopis and I. M. Tordesillas, in Encyclopedia of Electrochemistry of the Elements, Vol. VI (A. J. Bard, ed.), pp. 277-298, Marcel Dekker, New York (1976).
37. K. W. Lam, K. E. Johnson and D. G. Lee, Studies of ruthenium-oxy species in basic solutions by cyclic voltammetry, J. Electrochem. Soc., 125, 1069-1075 (1978).
38. L. D. Burke and D. P. Whelan, The behavior of ruthenium anodes in base, J. Electroanal. Chem., 103, 179-187 (1987).
39. F. Colom, in Standard Potentials in Aqueous Solution (A. J. Bard, R. Parsons and J. Jordan, eds.), pp. 413-427, Marcel Dekker, New York (1985).
40. Ref. 35, pp. 485-492.
41. T. F. Sharpe, in Encyclopedia of Electrochemistry of the Elements, Vol. I (A. J. Bard, ed.), pp. 235-347 (1973).
42. Z. Galus, in Ref. 39, pp. 220-235.
43. C. N. Welch, Pyrochlore electrodes, U. S. Patent 3,801,490, April 2, 1974.
44. M. R. St. John, Hydrogen production by biomass product depolarized water electrolysis, U. S. Patent, 4,395,316, July 26, 1983.
45. T. R. Felthouse, Catalytic oxidative cleavage of vicinal diols and related oxidations by ruthenium pyrochlore oxides: new catalysts for low temperature oxidations with molecular oxygen, J. Am. Chem. Soc., 109, 7566-7568 (1987).
46. O. Knop, F. Brisse and L. Castelliz, Determination of the crystal structure of erbium titanate, $Er_2Ti_2O_7$, by x-ray and neutron diffraction, Can. J. Chem., 43, 2812-2826 (1965).
47. P. C. Ford, J. R. Kuempel and H. Taube, The acid-catalyzed aquation of hexammineruthenium (II) and pentamminepyridineruthenium (II) complex ions, Inorg. Chem., 7, 1976-1983 (1968).
48. C. Cha, Wuhan University, Wuhan, People's Republic of China, personal communication.
49. M. S. Hossain, D. Tryk and A. Gordon, Pressure-tolerant air cathodes, 171st Meeting of the Electrochemical Society, Philadelphia, May 1987, Extended Abstracts, 87-1, pp. 466-467 (1987).
50. J. Prakash, D. Tryk, W. Aldred and E. Yeager, unpublished results.
51. L. B. Berk and D. Zuckerbrod, in: The Electrochemistry of Carbon (S. Sarangapani, J. R. Akridge and B. Schumm, eds.), pp. 238-250, The Electrochemical Society, Pennington, NJ (1984).
52. D. Tryk, W. Aldred and E. Yeager, in Ref. 51, pp. 192-220.
53. P. N. Ross and M. Sattler, The corrosion of carbon black anodes in alkaline electrolytes. III. The effect of graphitization on the corrosion resistance of furnace blacks, J. Electrochem. Soc., 135, 1464- 1470 (1988).